8-2015

Cell Impedance Sensing System Based on Vertically Aligned Carbon Nanofibers

Yongchao Yu
University of Tennessee - Knoxville, yyu6@utk.edu

To the Graduate Council:

I am submitting herewith a thesis written by Yongchao Yu entitled "Cell Impedance Sensing System Based on Vertically Aligned Carbon Nanofibers." I have examined the final electronic copy of this thesis for form and content and recommend that it be accepted in partial fulfillment of the requirements for the degree of Master of Science, with a major in Electrical Engineering.

<div align="right">Nicole McFarlane, Major Professor</div>

We have read this thesis and recommend its acceptance:

Gong Gu, Syed Islam

<div align="right">Accepted for the Council:
Carolyn R. Hodges</div>

<div align="right">Vice Provost and Dean of the Graduate School</div>

(Original signatures are on file with official student records.)

Cell Impedance Sensing System Based on Vertically Aligned Carbon Nanofibers

A Thesis Presented for the
Master of Science
Degree
The University of Tennessee, Knoxville

Yongchao Yu
August 2015

ACKNOWLEDGEMENTS

ABSTRACT

Standard biological assays are time consuming, occur at the end of an experiment, use bulky and expensive equipment and require skilled expertise. Lab on chip instruments seek to miniaturize these systems, improve ease of use and lower costs while offering real time measurements and accuracy. We have developed an electrical cell-substrate impedance sensing system using vertically aligned carbon nanofibers. The system is able to sense and measure biological cells' impedance in real time. By using carbon nanofiber arrays, the system is able to offer more sensitive measurements compared with traditional coplanar electrodes. This is the first demonstration of using vertically aligned carbon nanofibers (VACNF) to observe changes in cellular impedance. This work is not only an improvement over existing cell substrate impedance measurement systems, but also is an extension of carbon nanofiber application creating a new possibility for using VACNF in the bio-sensing area. At the same time, by using carbon nanofiber arrays, we have enhanced the possibility for integration of measurement system as a lab on chip system.

TABLE OF CONTENTS

LIST OF TABLES

LIST OF FIGURES

CHAPTER 1
INTRODUCTION

1.1 Cell impedance measurement system

Electrical cell-substrate impedance sensing (ECIS) has gained much interest in the biosensing arena. Biologists are interested in impedance sensing for both scientific and medical reasons [1]. This technique helps researchers in a wide range of applications such as medical diagnosis, cytotoxicity assessment, medical and pharmaceutical testing, and biochemical and environmental agent detection. ECIS has been used for cell attachment and spreading, cell proliferation, cell differentiation, barrier function, signal transduction assays, cell invasion, cytotoxicity, in situ cell electroporation and monitoring, cell migration and wound healing, cell chemotaxis, and cell – extracellular matrix (ECM) protein interactions. Figure 1 shows the principle of ECIS. An AC voltage is applied to coplanar electrodes. Between any two electrodes, there exists an electric field. Disturbance of the electric field will occur, as cells are introduced onto one of the electrodes, and results in a change of current and voltage. The ECIS system is based on following this principle. Now a days, a commonly used system in cell impedance measurement is to employ small planar gold film electrodes deposited on the bottom of cell culture dish and measure the impedance using impedance analyzers or lock in amplifiers [1].

Typical cell measurements use biochemical reactions to observe cellular changes. These can only (typically) be observed at the end of an experiment. ECIS is advantageous over these standard techniques in that it monitors the cells' behavior in real time and is a label free method. Thus a much richer dataset is possible using ECIS measurements to monitor cells. Additionally, because there are multiple electrodes, multiple populations of cells can be observed at any given time. However the ECIS system as employed in literature has severe drawbacks. The system, as seen in Figure 1, uses the planar gold electrodes. Current microfabrication techniques limit the size of these electrodes and commercially

available electrodes are typically on the order of 100-300 μm. The size of a cell is on the order of 5μm to 50μm, depending on the type of cell. Thus, it is difficult to get a one to one ratio of electrode to cell. Additionally, it could be advantageous to have multiple electrodes in contact with an individual cell. This is not possible using current microfabrication techniques. Planar electrodes are limited to approximately 10μm in size with a 10μm pitch.

This work, improves the resolution of current planar electrode arrays, by employing vertically aligned carbon nanofibers (VACNF) as electrodes. The use of these electrodes will provide increased resolution. Also, due to the physical nature of these nanostructures, the sensitivity of the impedance measurement will be increased.

Electric field lines go from one electrode to another

Electric field lines bent by presence of cell
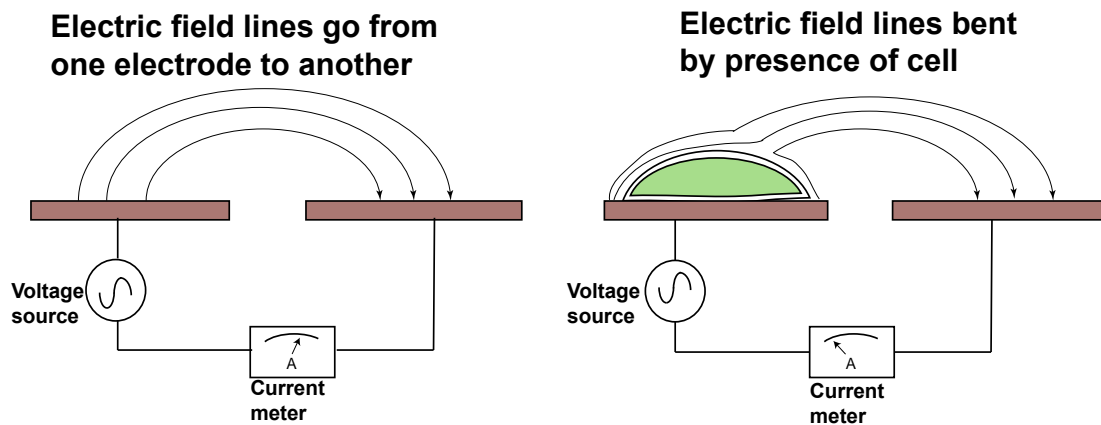
Figure 1. Overview of Impedance Sensing. The presence of a cell disturbs the electric field lines from between a pair of electrodes. This electric field disturbance translates into a change in measured current.

Figure 2. Commercially available gold film coplanar platform

Figure 2 shows the commercial product of gold film coplanar uses in ECIS. During the measurement, cells will be placed and cultured in each well on the platform. Cells will spread and attach to the gold layer on the bottom. By analyzing the voltage change, researchers are able to analyze the cells' behavior in real time. The approach is label free, meaning very little skill is required to use the system.

Figure 3 shows how the impedance changes for cell in different stages. When cells are first seeded unto a substrate (stage 1), they descend by gravity before adhering to the surface via biochemical processes (stage 2). This is correlated with an increase in impedance. During stage 2, there is a fluctuation in impedance over time due to the kinetic behavior of cells. Once the cells are adhered, they will respond to stimulants, both biochemical and mechanical, by undergoing cellular changes, such as membrane compromise, which will be reflected in a change in impedance (stage 3).
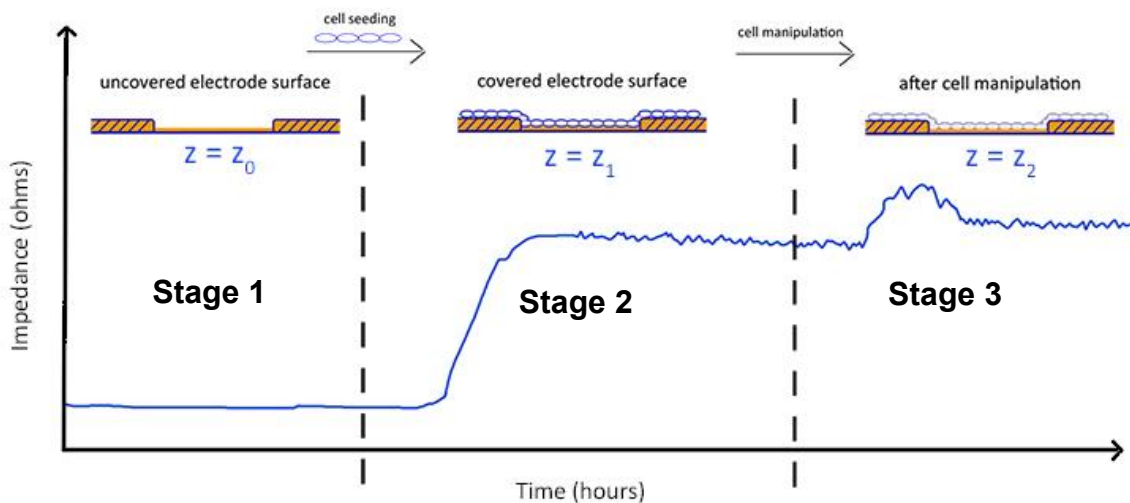
Figure 3. Impedance Change in as cell adhered to working Electron [2]

1.2 Nanotechnology

Nanotechnology has shown rapid development in recent years. In bioresearch, nanotechnology has opened many new research avenues for biologists due to the small size, tailoring ability, and multi-functionality of nanoparticles [3]. There are many application of nanotechnology have been introduce by researchers in very wild area, such as pH sensor [4], gas sensor [5], and also in many biological applications [6] [7]. For the vertically aligned carbon nanofibers (VACNF), due to their excellent structural and material properties, we believe that VACNF could become a novel biosensing platform for cells and other biological molecules. VACNF has many irregularities and defect sites as a function of its unique structural properties. This allows improved immobilization of enzymes. This also offers a highly conductive path to external pads. As another property, the VACNF electrodes have been reported as high electron field emitters [8]. These properties can enhance the sensitivity of the planar electrode pattern and allow the VACNF electrodes to become novel candidates for biosensing applications. The size of carbon nanofibers allows for the high resolution measurements. The

4

diameter a single of VACNF is approximately 100 nm. In our case, the diameter for each single fiver is in the range of 80 nm to 150 nm. Compared with the size of a cell, which is around 1 µm -100 µm for different type of cells. Therefore, for each cell, there will be multiple VACNF electrodes in contact with it.

In this master's thesis we have designed and fabricated a VACNF platform to replace the coplanar electrode platform in the traditional electric cell substrate impedance measurement system. The VACNF electrodes have very outstanding characteristics and structure, and this will increase the sensitivity and resolution of the measurement system.

1.3 Thesis Organization

The thesis is organized as follows. Chapter 2 surveys the literature on electric cell substrate impedance sensing and vertically aligned carbon nanofibers. Chapter 3 discussed the Vertically Aligned Carbon Nanofibers (VACNF) platform fabrication process including the PECVD method, component analysis, multiphysics simulation using COMSOL and equivalent circuit model for SPICE simulations. Chapter 4 discusses the custom measurement system setup and cell culture process, as well as transferring of cells to the measurement platform. Chapter 5 gives the results of the measurement system with standard RC circuits and of the VACNF with Bovine Aortic Smooth Muscle cells. Chapter 6 gives the thesis conclusion and outlines areas of future work.

CHAPTER 2
LITERATURE REVIEW

2.1 Electrical cell-substrates impedance sensing

The first idea of ECIS come up in 1980s, by Dr, Ivar Giaever who was working at General electric Research Laboratory in Niskayuna NY [9]. He was joined by Dr. Charles R. Keese who worked with him on a national science foundation grant. As researchers with a physics background, they were interested in the effects of electromagnetic fields on biological cells. In early experiments, Dr. Giaever and Dr. Charles applied a DC (time invariant) voltage to cells adhered to two electrodes. After the test, they found that the cells were dead on one of the electrodes. The reason for this problem due to electrochemistry and the high currents leading to ionization and not because of the high DC voltage. The problem was solved by applying an AC voltage. In the first ECIS system, a 1V AC signal was applied at 4 KHz, through a 1MΩ resistor. The current was limited by the 1MΩ resistor, and an approximate constant current of less than 1 μm was applied to the electrodes. This became the standard measurement architecture in today's ECIS system. As another contribution, Drs. Giaver and Charles' research group found the relationship between the solution resistance or constriction resistance changes and the radius of a circular working electrode.

$$R \text{ (solution)} \sim 1/r$$

By reducing the electrode radius, the electrode resistance can be made dominant over the solution resistance. Therefore, in today's ECIS system, the diameter of the working electrode is designed around 250 μm. This is large enough to contain a sizable population of cells and small enough to have a relatively small constriction resistance

In 1998, a very important paper of using ECIS to study cells interactivity was published by L. Reddy *et. al* [10]. In this paper, the author used ECIS to monitor human orbital fibroblastic cells after introducing prostaglandin and leukoregulin. These two types of drugs have a similar effect on cells. As the result of real time

ECIS, they were able to note that the cells had an immediate impedance change response with prostaglandin. However, it took 2 hours for the cells to responsd to leukoregunlin. The reason for the late response of the cells is that they had to synthesize proteins before they could respond [11]. This experiment shows that for different kind of drugs, cells show different response speeds. This helps to distinguish the drugs and study the cellular activity.

As the development of the ECIS technology has progressed, there have been many commercial products developed. Figure 4 shows a few of the standard electrode arrays. They range from circular to interdigitated and from one electrode to many electrodes. In the model this thesis uses for comparison,, there are 8 wells containing a single circular active electrode. The diameter for each electrode is 250 µm. The maximum volume for each well is 600 µL. 50-100 cells can measure for each well. Figure 5 shows the schematic for each measurement unit. The white dot in the center is the working electrode which has 250 µm diameter, the gold circle sounding it is the interconnection. In this sample, gold is used as the material of interconnection. There is a ground electrode, common to all eight active electrodes, placed on the center of platform.
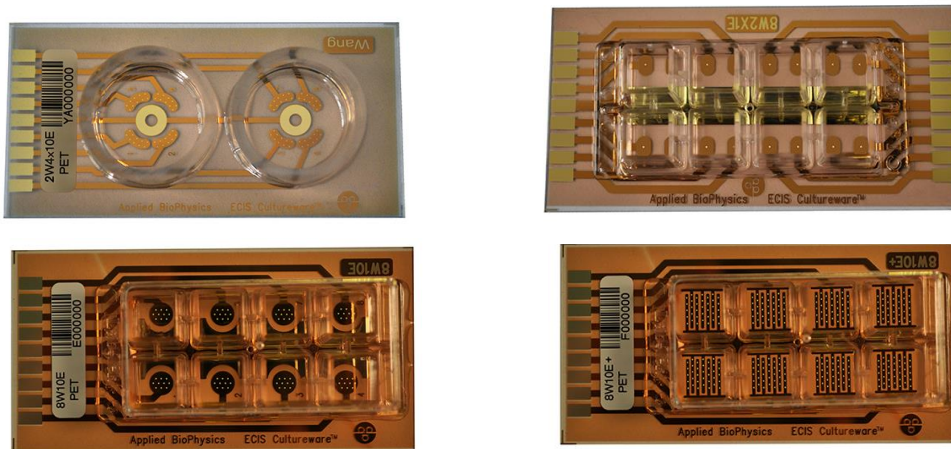
Figure 4. The electrode array model from Applied Biophysics **[2]**. These arrays range from single pairs of electrodes to interdigitated electrode architecture

Figure 5. Schematic of each measurement unit of one of the electrode arrays **[2]**

Today, ECIS already become an importance technique in bio-sensing and biology area. There are many application that have been developed. These applications include immunological response models, Insight into mechanisms of all phases of cell growth and reproduction, real time monitoring of cells in culture, cell-substrate interactions, and cell sorting. The immune response to stimulations has been reported for cells such as epithelial and endothelial lung cells [12] [13]. These responses typically include blood coagulation activation, immune cell and cellular morphology changes. For example, thrombin induces change in cells' shape, cell-cell adhesion decreasing and release cytokine from endothelial cells and the ticin from Stachybotrys chartarum (an environmental contaminant) has been reported to induce changes in cell morphology and release of the inflammatory cytokine, Interleukin-8 from A549 cells [14] [15]. Studying the dynamic response of cells as they settle and adhere to the surface [16] [17] will help the study the cell adhesion and decision processes and become key to new genetics discoveries. Also, in stem cell studies, insight into cell differentiation can be one of the most significant studies, which will have a large potential boarder societal impact [18] [19]. Monitoring neuronal cells' activity will help in understanding the brain-machine interfaces. It would enable the studies of wound healing of a destroyed/impaired monolayer of cells and it could lead to the better understanding of how the cells repair themselves. Also by monitoring cell to cell contact that may inhibit or promote certain cell proliferation [20] [21]. These studies

8

could also be extended to bacteria or viruses and other molecular studies. Monitoring the motility and spreading of cells with different substrates will enable studies of cells' interaction. This will is useful for determining the activation of cells on different proteins, for example, bovine serum albumin, gelatin bovine fetuin, or human plasma fibronectin [22]. Also it is useful in quantitative analyses of the interaction of cell and/or tissues with various macro and nano-particles or substrates. For example, this could help in studies in using networks of living neurons. It also could be used to understand how different organs work, such as using printing technology currently available to create organs. These characteristics are also useful for selective counting of a specific cell within a mixture of cells [23] [24].

2.2 Vertically Aligned Carbon Nanofibers

The history of carbon nanofiber could be traced back to 1889 [25]. It was reported that carbon filaments are gases from carbon-containing gases using an iron crucible. However, due to the limitation of microtechnology in the early years, the development of nanofibers progressed very slowly. In the 1950s, as the development of high resolution electron microscopy came into being, the transmission electron micrographs of nanofiber was obtained by Radushevivh and Lukyanovich [26]. In 1990s, the discovery of C^{60} lead to abroad interest in carbon nanofiber and nanotube.

The Plasma enhanced chemical vapor deposition (PECVD) process was introduce by Chen *et. al.* in 1997 [27]. In this paper, they successfully fabricated carbon nanostructures on Silicon substrates using the PECVD process. This process lead to the development of nanostructure synthesis. It allows researchers to have better control over the position, alignment, diameter, length, chemical composition, and other characteristics of individual nanostructures.

9

Mekechko *et. al.* reported vertically aligned carbons nanofiber and its synthesis process in 2005 [28]. Carbon nanofibers are defined as cylindrical or conical structures that have diameters from a few to hundreds of nanometers, and lengths ranging from less than a micron to millimeters. In this paper, Mekechko introduced that the internal structure of the carbon nanofiber varies and is comprised of different arrangements of modified graphene sheets. Figure 1 shows the internal structure of carbon nanofiber.

According to Mekechko *et. al.*, a graphene layer can be defined as a hexagonal network of covalently bonded carbon atoms. In general, nanofibers consist of stacks of curved graphite layers that form "cones" or "cups", as shown in figure 6 (b). Angle alpha is defined as the angle between the fiber axis and the graphene sheet near the sidewall surface. In the very special case where $\alpha = 0$, one or more graphene layer from the cylinder runs the full length of the nanostructure. This type of nanofiber is called nanotube (CNT).
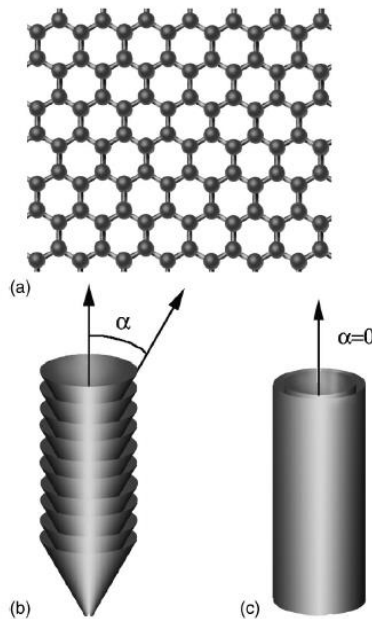
Figure 6. Structure of carbon nanofiber and nanotube
(a) Graphene layer (b) stacked cone nanofiber and (c) nanotube **[28]**

As the one of the property of carbon nanofiber, it has been reported as an electron filed emitter [29]. M.A. Guillorn *et. al.*, reported a gated field emitter using a single VACNF as the field emitter cathode. According to Guillorn *et. al.*, the dives could achieve significant operating current for extended period of time without causing degradation the VACNF tips.

There have been many reported applications of VACNFs. These include bio-chemical sensor and nervous system sensing. Using VACNF in bio-sensors was reported as an important application of VACNF, including as am enzymatic amperometric biosensor [30], and amperometric bienzymatic glucose biosensor [31]. The VACNF was reported as an effective strategy in biosensor, due the unique structural properties. The defect sites show not only high immobilization ability, but also show strong electrical current response. As application of VACNF in nervous system sensing, electrophysiological signals sensor [32] and dopamine and serotonin sensor have been reported [33]. As the advantage of using VACNFs, sensitive has been improved, also the carbon based electrodes have potential advantages over metal electrodes. This has contributed to precise, informative, and biocompatible interfaces.

CHAPTER 3
VERTICALLY ALIGNED CARBON NANOFIBERS (VACNF) PLATFORM FABRICATION PROCESS

3.1 PECVD

Plasma enhanced chemical vapor deposition (PECVD) technique was used in this thesis to fabricate the carbon nano-fibers. This is a commonly used process in nano-fiber fabrication, and has been reported in many publications [34] [35]. Quartz substrate was used. The Quartz substrate shows excellent chemical resistance with high stability against a variety of solvents. Also it has great heat resistant with high dimensional stability over a wide temperature range. For the most important characteristic, it is a transparent substrates, therefore the cells are able to be viewed under inverted microscopes.

During PECVD process, the chamber will be heat up to 700 ° C. Therefore a material that has a high temperature resistance is required for use as the substrate. Quartz has excellent chemical resistance and very high dimensional stability over a wide temperature range. 1000 **Å** Titanium (Ti) layer was placed on Quartz layer as the interconnection layer for the platform. Before the PECVD process, a thin layer of Chromium, Cr, was deposited over the wafer as a conducting surface. This Cr layer will act as a cathode during the PECVD process. 300 nm diameter and 50 nm thick Nickel (Ni) dots was placed on the top Quartz substrate by using conventional electron-beam lithography [28]. VACNF will growth on the place where the Ni dots was placed. Figure 7 shows detail of PECVD process.
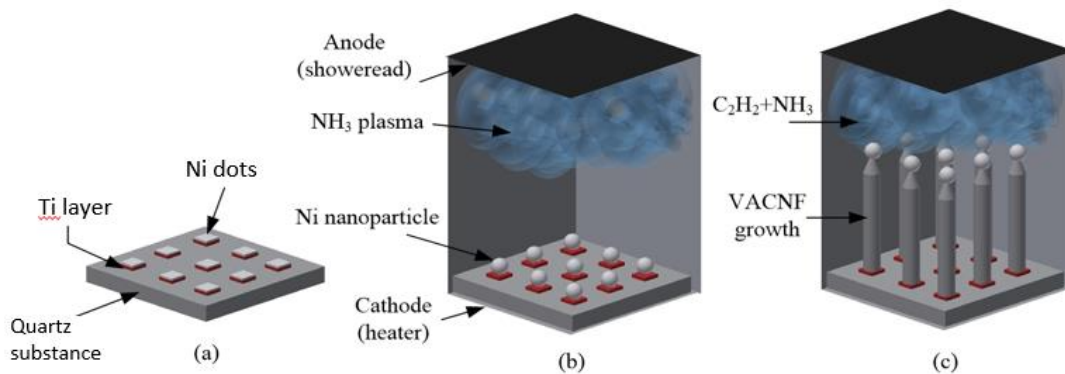
Figure 7. Detail of PECVD process

In the PECVD process, after a wafer was placed into the reaction chamber, the reaction chamber was heated to 700 ° C, and the pressure inside of chamber was reduced to 10-5 Torr, which is close to vacuum environment. Low reaction pressure helps the fibers to grow more uniformly. After achieving the condition mentioned above, ammonia (NH$_3$) plasma was gently introduced from shower head, which is located on the top of chamber. This treatment will reform the deposited catalyst nanoparticles (Ni particle) to discrete catalyst. The catalyst nanoparticles act as the seed of VACNF and with the specific thickness and diameter that mentioned above, only a single nanoparticle is formed from each catalyst dot [28]. As the next step, acetylene (C$_2$H$_2$) was introduced to chamber. This will growth VACNF immediately. The reaction time is approximately 20 min. After the PECVD process, the Cr layer was removed. Reaction time length, size of Ni dots and speed of ammonia plasma and acetylene are introduced, all these factors will have effect on the growth of fiber. Generally speaking, the longer reaction time creates longer nanofibers. However, if the time is too long, the reaction could break the fiber that has already been grown. In the conditions above, the length of fibers that have been successfully grown is around 3.5 μm to 7 μm with 80 nm - 110 nm diameter

13

3.2 VACNF platform

Figure 8 shows the fabricated VACNF platform. The size of the platform is 4 cm X 4 cm. And a total of 8 measurement units are fabricated on a single platform. There is one reference electrode, which is 0.2 cm in width, interconnection and eight active electrodes with 300 µm diameter. Each active electrode is circular in shape. Figure 9 shows a single measurement unit, (a) VACNF, (b) interconnection, (c) Ground. Ti was used as interconnection in this platform. This VACNF platform was design to replace the coplanar electron array produced by Applied Biophysics. Therefore a similar pad structure has been used. Figure 10 shows the schematics of a single measurement unit from applied biophysics. The diameter of the working electrode from one of the electrode arrays from applied biophysics is 250 µm. In our platform the working electrode was replaced by VACNF with 300 µm diameter.
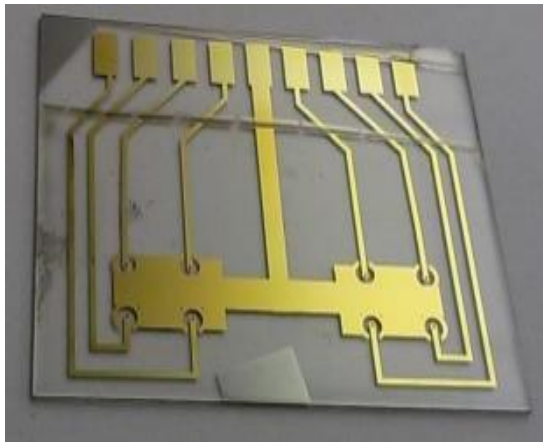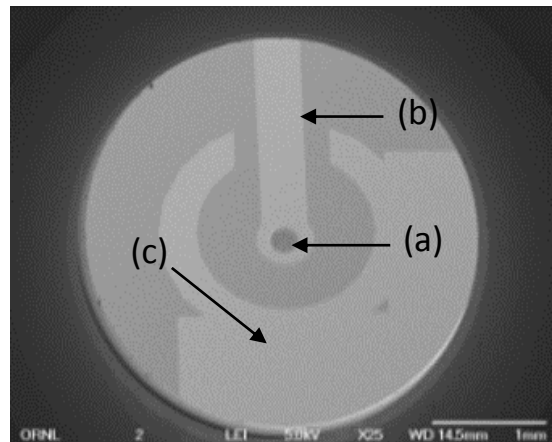

Figure 8. VACNF Platform.

Figure 9. VACNF Platform Measurement Unit

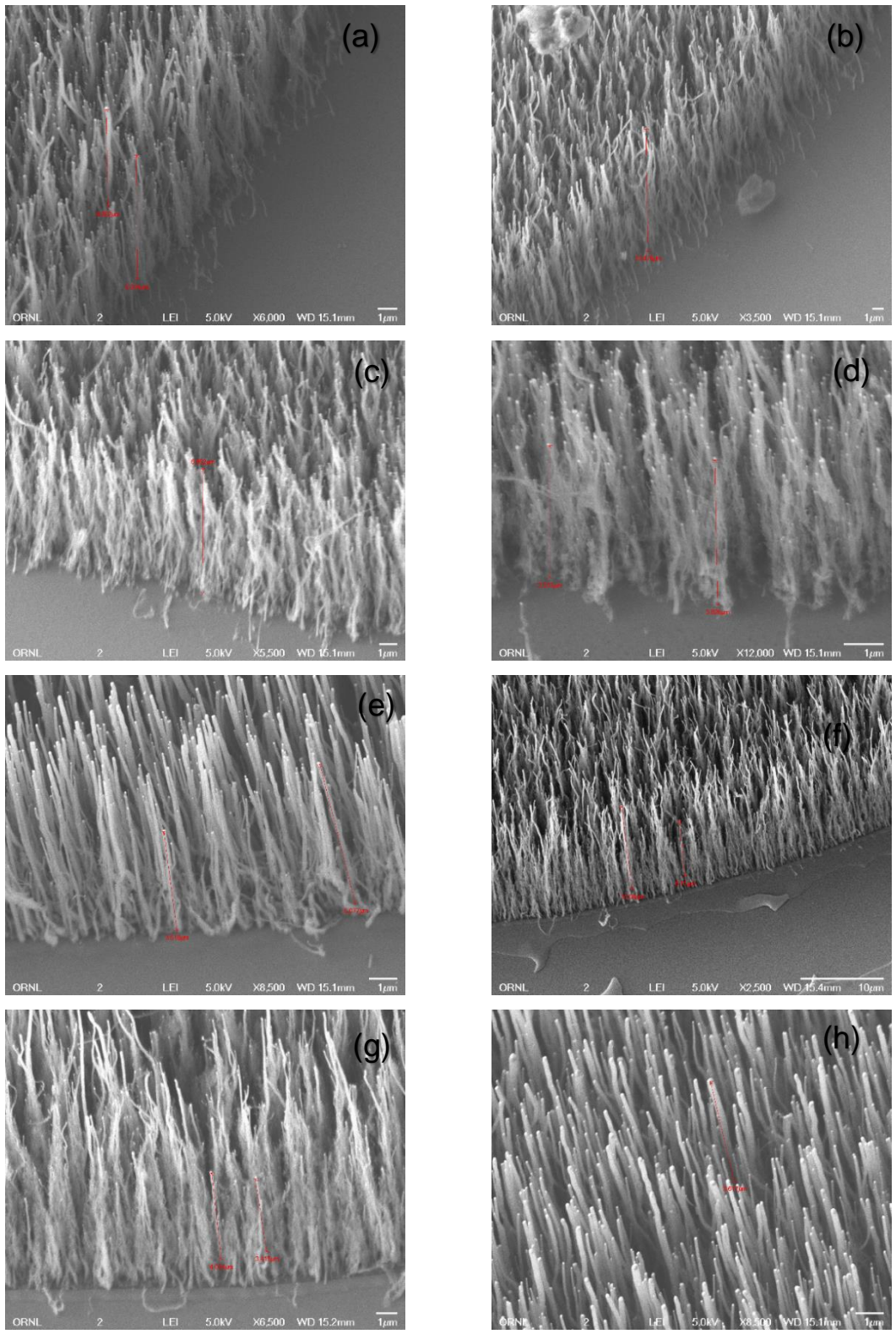Figure 10. Schematic of measurement unit

Figure 11. (a)-(h) SEM image of VACNF for different samples

Figure 11 shows the image of the fabricated VACNF under scanning electron microscope (SEM). These samples were fabricated under the conditions previously described. Table 1 shows the length of the carbon nanofibers in the different samples. Even though all the VACNF were at strictly controlled conditions, it is very obvious that length of fibers have more or less individual differences. The length of carbon nanofibers are in the range of 3.4 µm to 10 µm.

Table 1 Length of Nano-Fiber

Sample	A	B	C	D	E	F	G	H
Fiber length (µm)	4.892	10.475	6.852	3.313	3.516	6.711	4.034	3.617
	6.234			3.626	5.071	10.09	3.416	

Figure 12 shows the image of VACNF forest for each single measurement unit. The diameter of VACNF forest was designed to be 300 µm. The size of each VACNF forest are shown on Table 2. As a result, the diameters of VACNF forests very close to the designed size. From figure 12, we can observe that in some of samples, the VACNFs show fractures or folds, the main reason for this phenomenon is due to the alignment of Ni dots. Because of the very narrow size of the VACNF, it is very difficult to align the Ni dots perfectly. Once the Ni dot was placed on outside of designed regions, it will cause a fracture or fold on the VACNF forest.
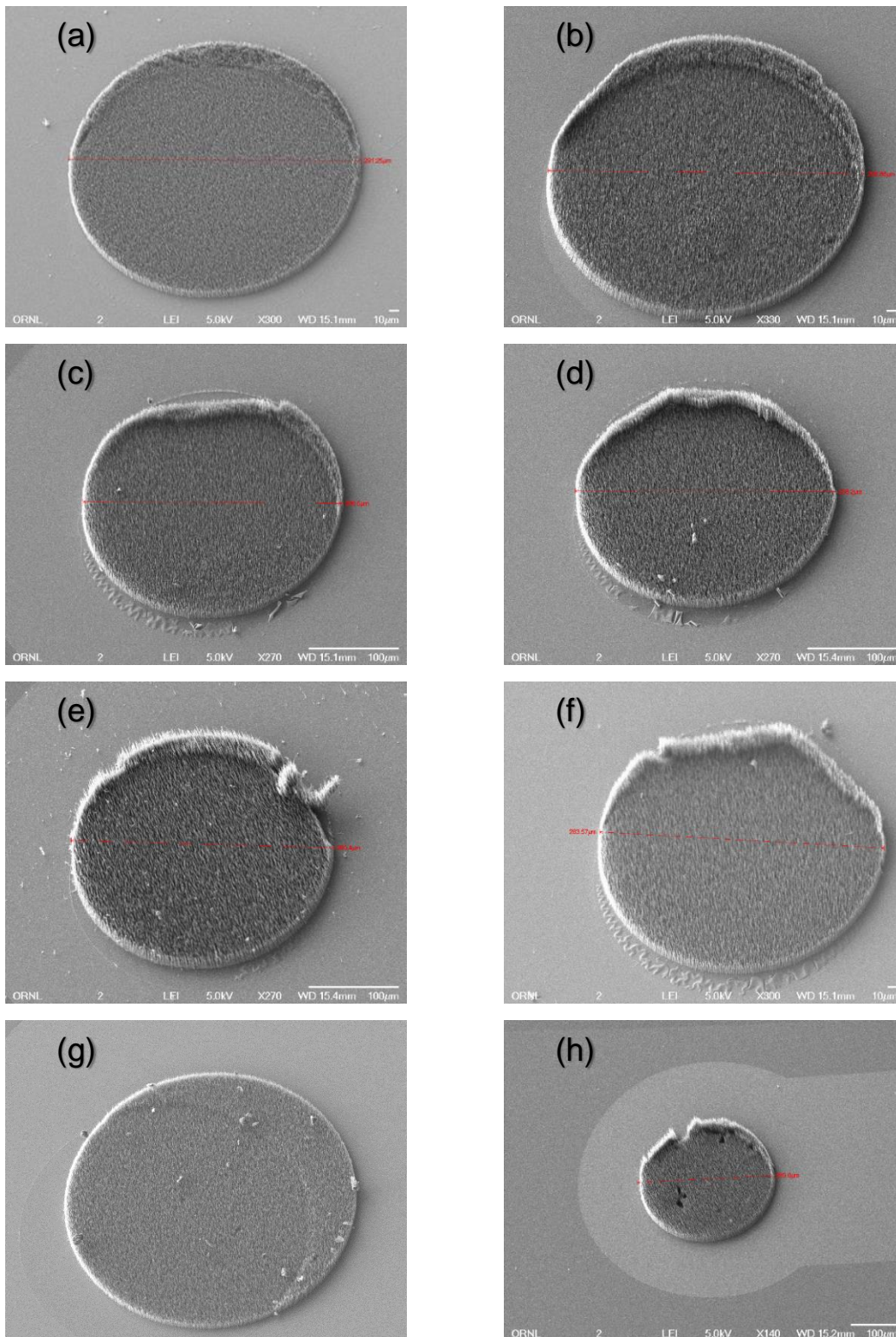
Figure 12. (a)-(h) Image of Single Measurement unit

Table 2 Diameter of Singale Measurement unit

	a	b	c	d	e	f	g	h
Diameter (μm)	291.25	286.66	286.5	288.2	290.4	283.57	291.56	289.0

3.3 Passivation layer fabrication and results

After fabrication of the first prototype of VACNF platform, a passivation layer was added on the top of platform to cover the interconnection layer and only allow the VACNF to be able to contact with cells. As per the developed process, before the Ni dots were placed on the Ti layer, a 200 Å SiO_2 layer was placed on the top layer and only left small gaps where the Ni dots were planned to be placed. Figure 13 shows the image of a single VACNF measurement unit with passivation layer. As shown on figure 13(d), there are still a few Cr particle left on the platform. After PECVD process, Cr layer is supposed to be etched out, however, the passivation layer will be also etched out, if the process time was too long. In our case, the process time was reduced to 20 sec. In previous work, which is a platform without passivation layer, it was 1 min. Because of the short acting time to protect the passivation layer, there is some Cr particle left on platform.

As one of the problems, in some samples, after PECVD process, the interconnections show obvious damage. Figure 14 (a-d) show the picture of the damaged interconnections. This problem only happens after placing the passivation layer on the platform. The process is the same as describe earlier in the thesis. Most of the interconnections damage occur where there is no covering by passivation layer. A possible reason for this problem is that, in our sample, the passivation layer was not covering the whole interconnection and/or the ground was not covered by SiO_2 layer. Thus during the PECVD process, the platform was unevenly heated. This most likely caused the intersection damages.

Figure 13. Image of a single VACNF measurement unit with passivation layer
(a) VACNF, (b) interconnection (c) passivation layer (d) Cr particle

As one of the problems, in some samples, after PECVD process, the interconnections show obvious damage. Figure 14 (a-d) show the picture of the damaged interconnections. This problem only happens after placing the passivation layer on the platform. The process is the same as describe earlier in the thesis. Most of the interconnections damage occur where there is no covering by passivation layer. A possible reason for this problem is that, in our sample, the passivation layer was not covering the whole interconnection and/or the ground was not covered by SiO_2 layer. Thus during the PECVD process, the platform was unevenly heated. This most likely caused the intersection damages.
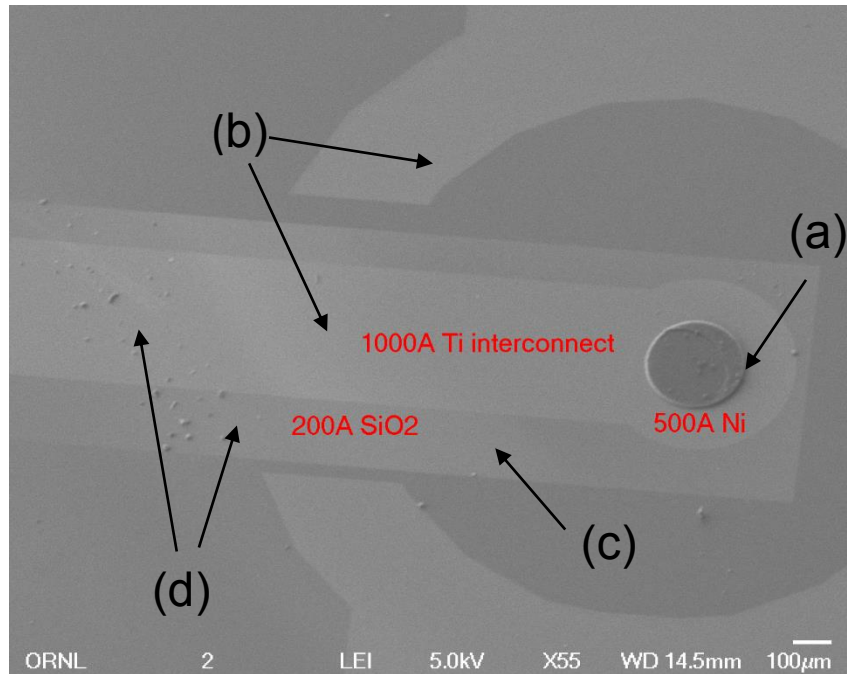
Figure 14. Damaged Interconnections on Samples

Another problem that occurs is the displacement of the VACNF. This is mainly due the ailment of Ni nanoparticle. The Ni particle was supposed to be placed on the Ti layer. However, after passivation layer was introduced, the space for Ni placement was much narrower than without the passivation layer. This significantly increased the difficulty of Ni placement. In some cases, Ni particles were mismatched with the designed place. Part of the Ni particles were placed on SiO_2 passivation layer. As a result, some of the VACNF samples show fracture or fold. And also this will cause the damage on interconnection as well.

Where the edge supposed to be as design

VACNF Edge

ORNL   2   LEI   5.0kV   X900   WD 15.2mm   10μm
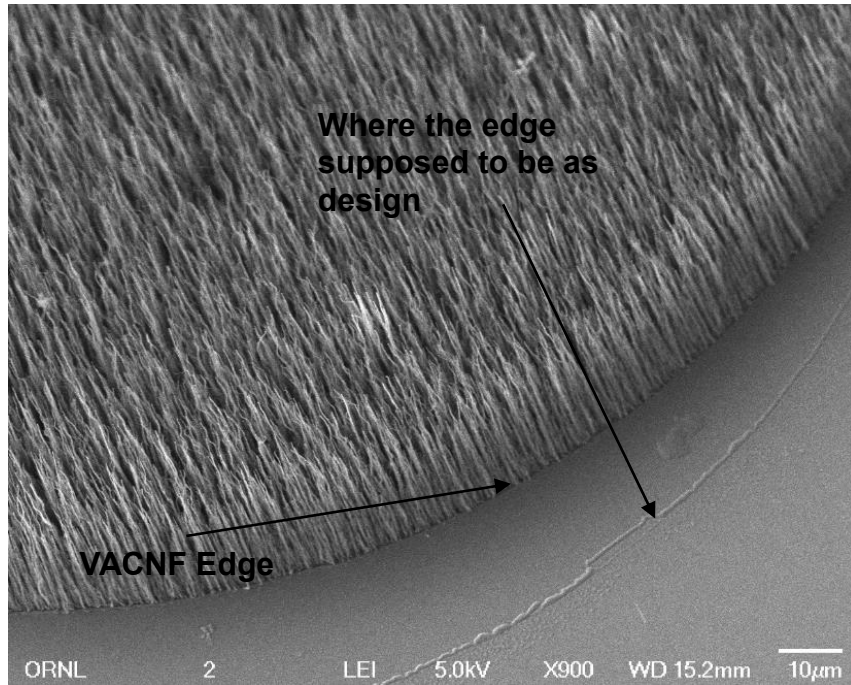
Figure 15. VACNF Mismatched with Designed Place.

Interconnection Damage

Fracture of VACNF
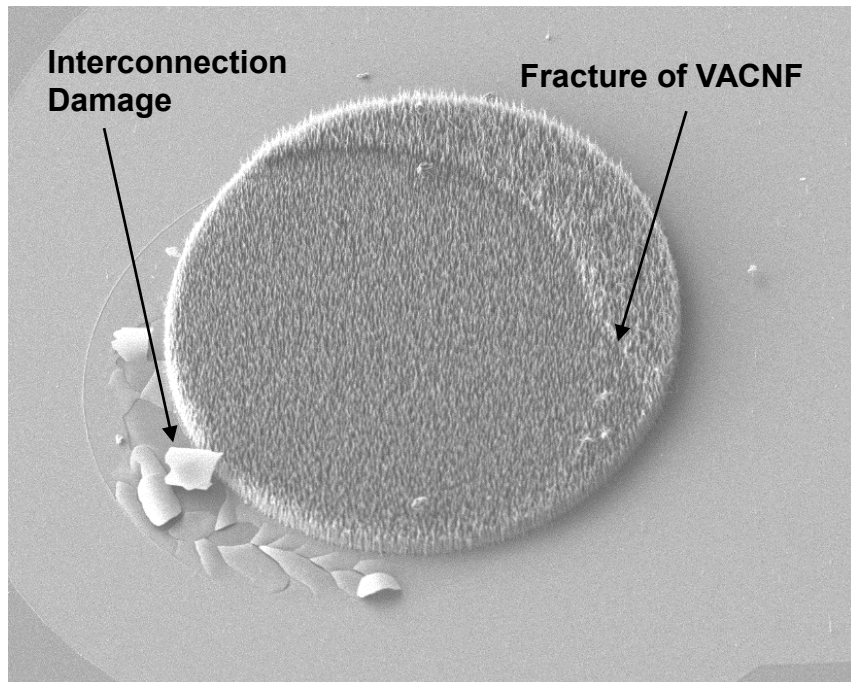
Figure 16. Damaged VACNF and Interconnection I
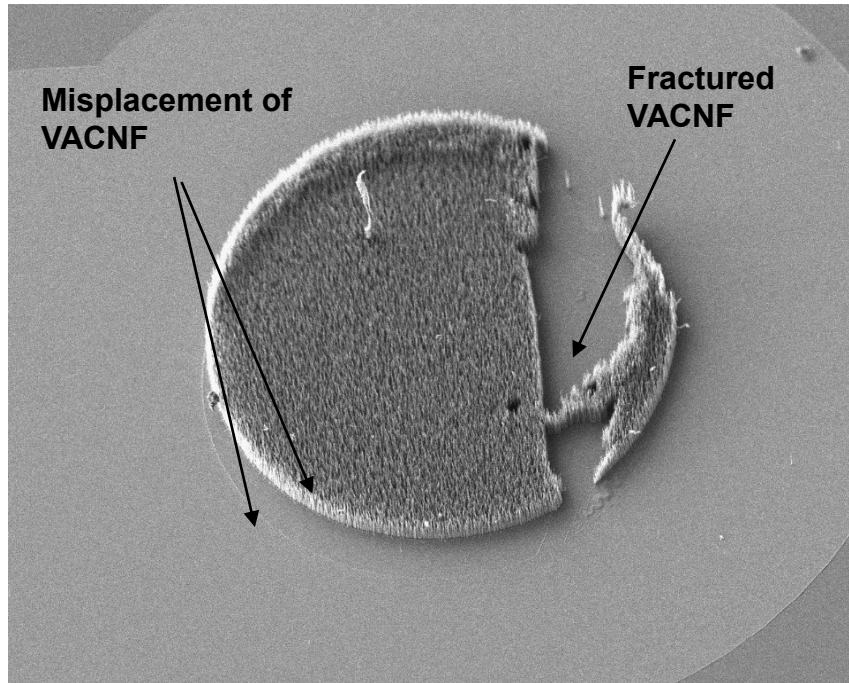
Figure 17. Damaged VACNF and Interconnection II

3.4 Component Analysis for VACNF Platform

After the fabrication of the VACNF platform, component analysis was performed by taking an energy-dispersive x-ray spectroscopy (EDS) elemental analysis. The EDS analysis include the generation of an X-ray from the entire scan area of the SEM [36]. Figure 18 shows the SEM image for elements C, O Si, Ti and Cr. The different colors represent deferent element.

Figure 18. SEM Chemical Composition Image for Platform
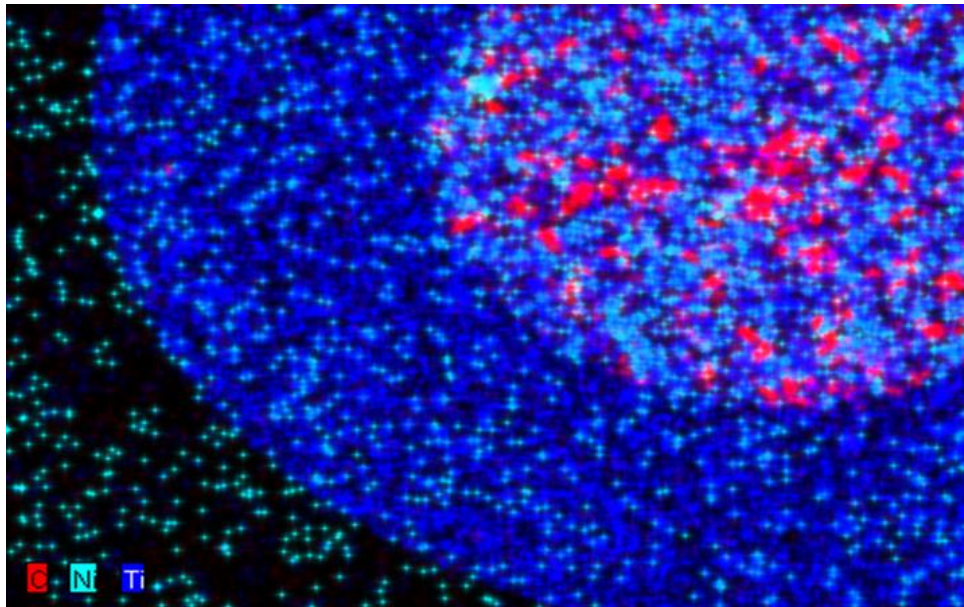
(a) Platform under the SEM chemical composition image for C, Ni and Ti
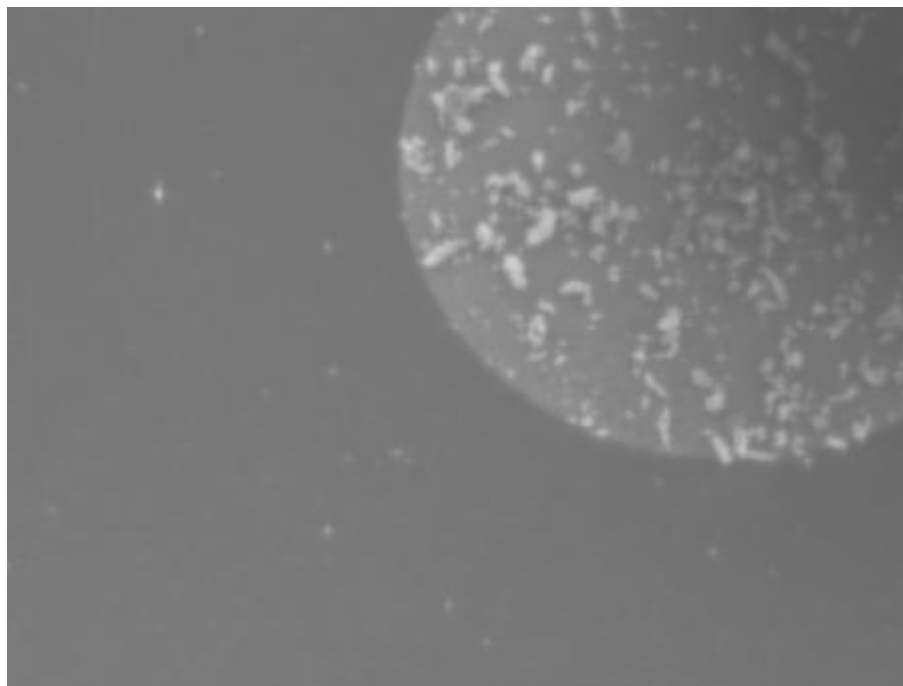
(b) Image of platform under SEM

Figure 18. Continue
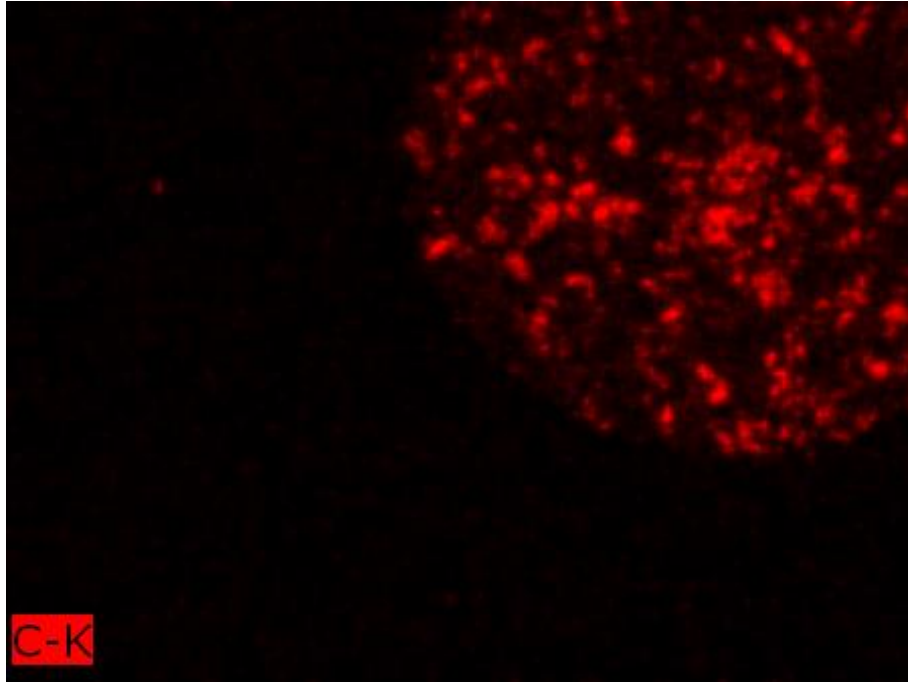
(c) Carbon under the SEM chemical composition image
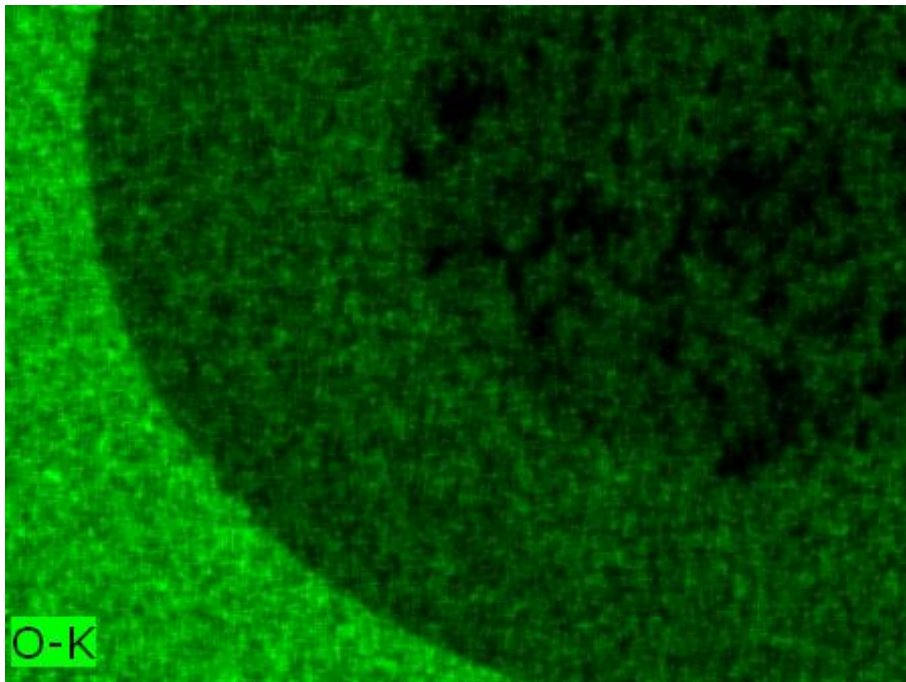
(d) Oxygen under the SEM chemical composition image
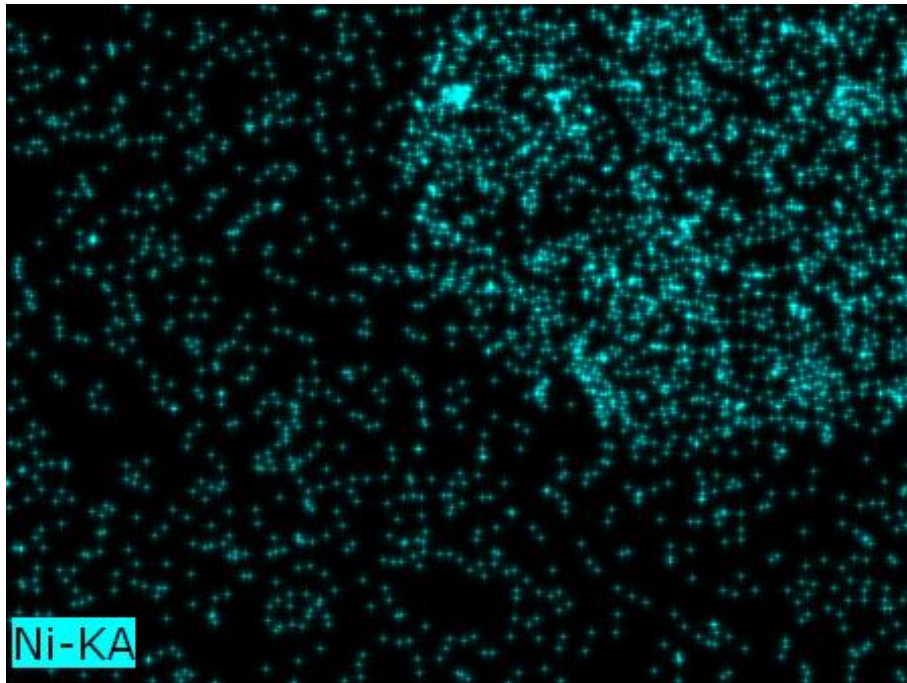
Figure 18. Continue

(e) Nickel under the SEM chemical composition image
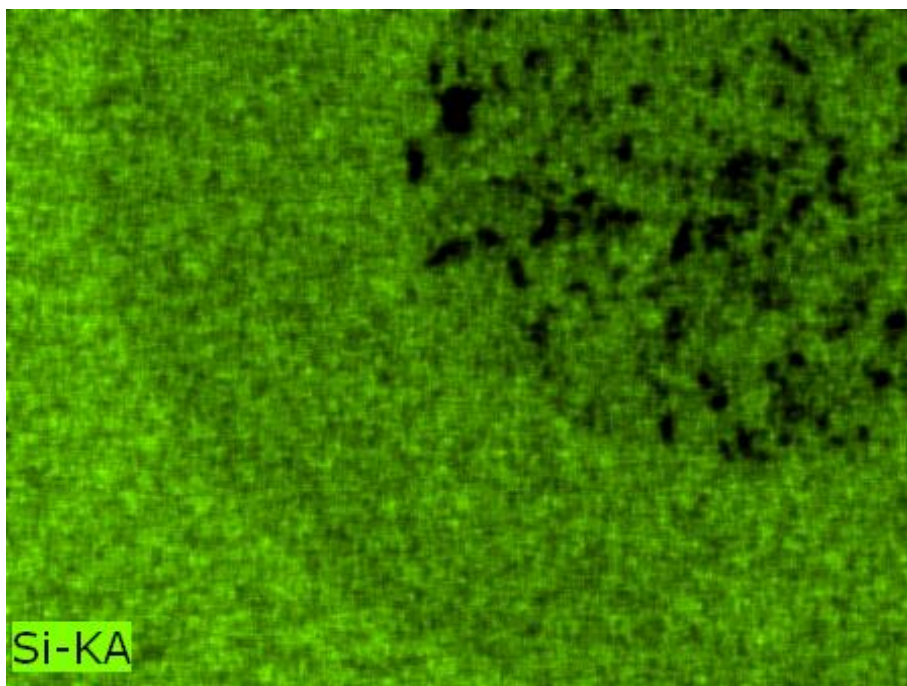
(f) Silicon under the SEM chemical composition image
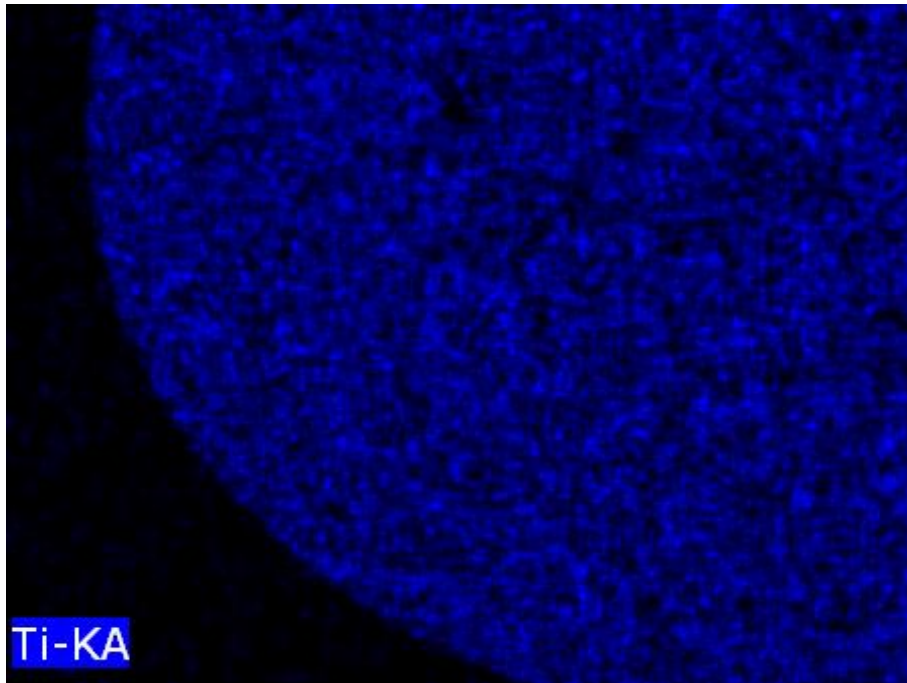
Figure 18. Continue

(g) Titanium under the SEM chemical composition image
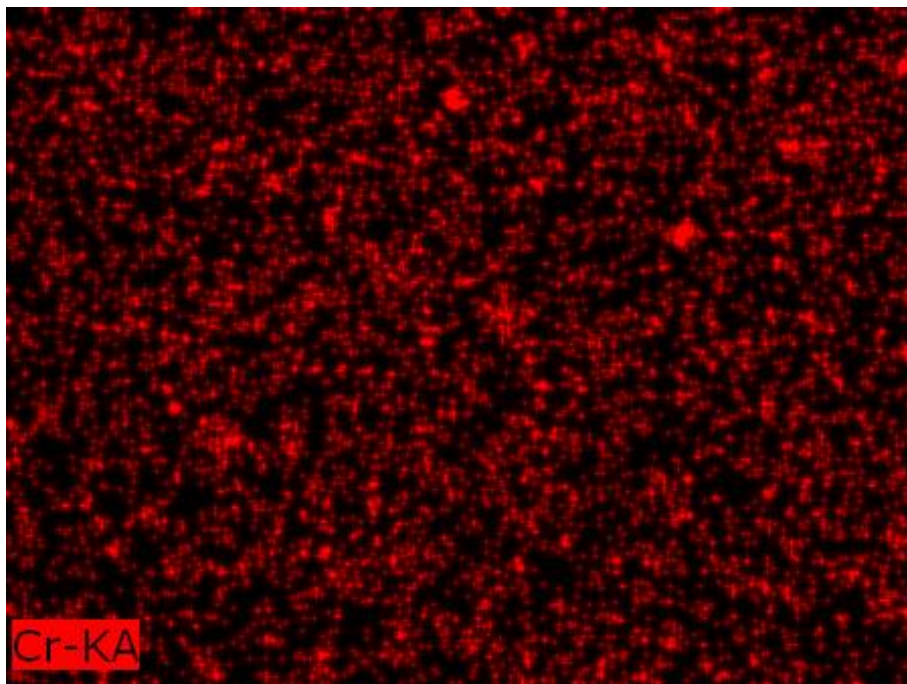
(h)Chromium under the SEM chemical composition image

Figure 18. Continue

There are 5 elements has been find from VACNF platform. Table 3 shows the SEM Spectrum Data for each element. Carbon element is mainly introduced by carbon nanofiber, which take the main component in VACNF platform. Oxygen and silicon is comes out of the Quartz substrate. Titanium is from the interconnection. The results shows that there are still a small amount of Nickel left on the VACNF. Figure 19 shows the EDS elemental analysis of each element distribution. The Y-axis shows the counts (number of X-rays received and processed by the detector) and the X-axis shows the energy level of those counts [36].
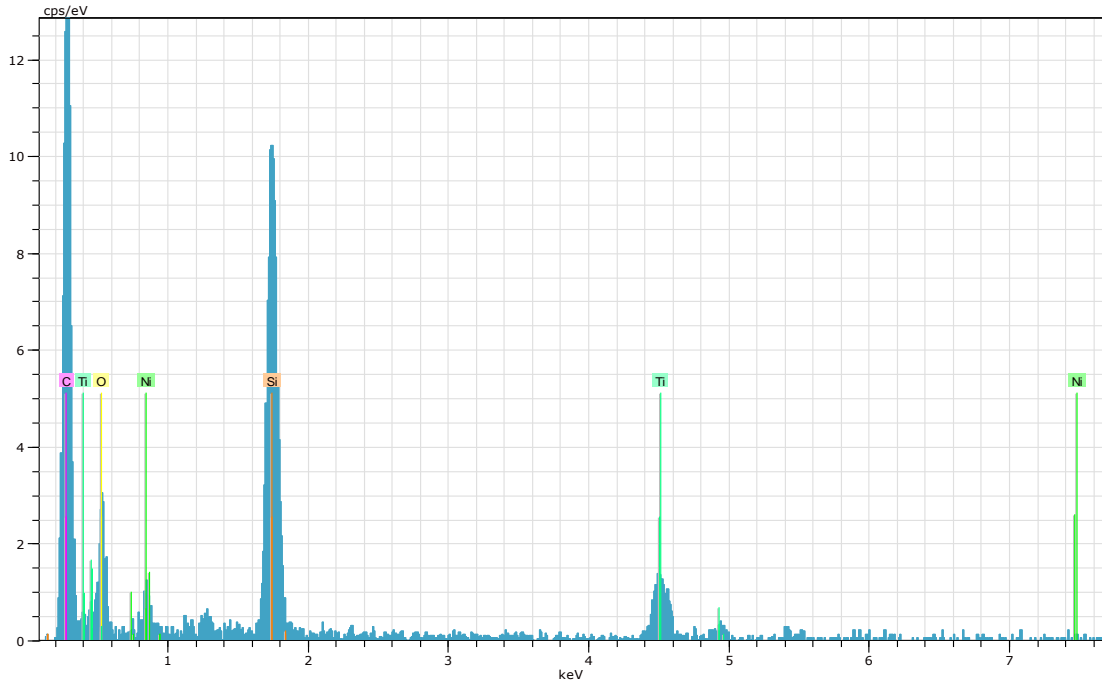
Figure 19. Distribution Diagram for Elements

Table 3 SEM Spectrum Data

Element	Series	unn.C [wt %]	Norm c [wt. %]	Atom.C [at. %]	Error [wt.%]
Carbon	K-series	66.885	55.77	71.94	12.18
Oxygen	K-series	15.92	15.89	15.92	5.80
Silicon	K-series	15.74	15.71	8.66	0.92
Titanium	K-series	11.34	11.32	3.66	0.87
Nickel	K-series	1.31	1.31	0.35	0,48

3.5 Simulation using COMSOL

For the purpose of explaining that using VACNF could improve the sensitivity of measurement from view of the physical structure, a simplified physical model was developed and simulated in the COMSOL program. COMSOL is a finite element analysis tool. Figure 20 shows the simulation result for coplanar electrodes and the VACNF platform. Some assumptions have been made. First, we approximate that shape of a cell is a unit elliptical shape. Arrayed triangles are used to represent the VACNFs. This is similar to the shape of VACNFs. Carbon material was selected as the material properties of VACNF, which is the same material as the VACNF. For both coplanar and VANCF, interconnections were set as Ti, which is the same material in the fabricated VACNF platform. Instead of modeling the Bovine Aortic Smooth Muscle cells, we used a muscle cell model, which is a built-in model in COMSOL. The values of the dielectric properties of the cell were edited to match our chosen cells. The property details are show on table 4 – table 6. Input voltage potential was 1V. An active central electrode with two

planar ground electrodes are assumed as the structure. Color in the figure 20 shows the strength of voltage potential and line shows electrical field.
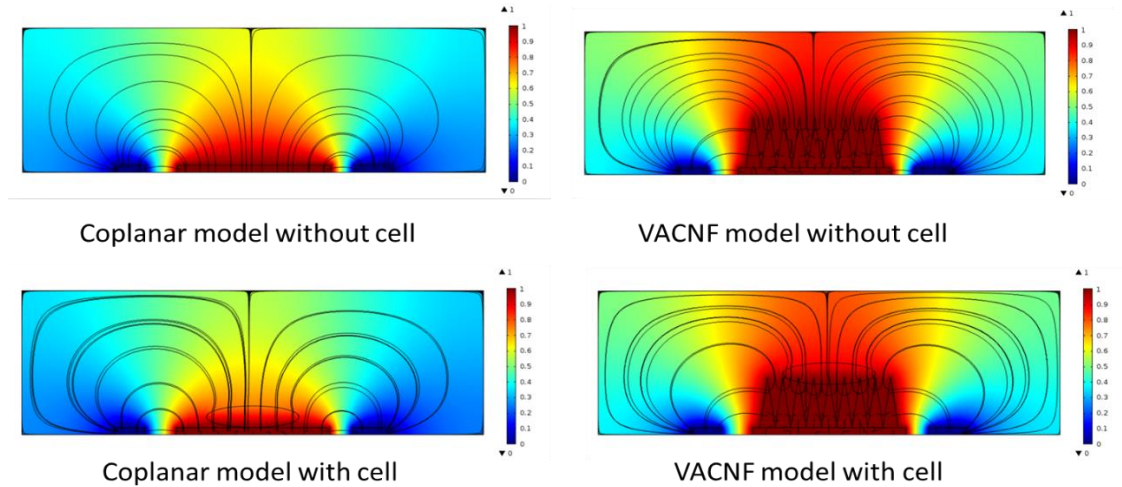
Figure 20. Simulation Result for Coplanar Model and VACNF Model

In simulation results, the VACNF model shows stronger voltage potential than coplanar electrode model. The electrical field is define as:

$$\mathrm{E_x} = -\frac{dV}{dx}$$

Where Ex is the electrical field in x-detraction, dv/dx is the gradient of the electric potential in the x-direction. Therefor more concentrated electrical field line could be observed from VACNF model compare with coplanar model. This represents that for same amount of impedance change, the VACNF model will show larger potential change which means VACNF is more sensitive in impedance change than coplanar model.

Table 4 Property of Smooth Muscle cell

Property	Value	Unit
Relative Permittivity	20	
Heat capacity at constant pressure	3421	J/(Kg*k)
Density	1090	Kg/m^3
Thermal Conductivity	0.49	W/(m*k)

Table 5 Property of Titanium beta-21s

Property	Value	Unit
Relative permittivity	86	
Relative permeability	1	
Electrical conductivity	7.407e5	S/m
Coefficient of thermal expansion	7.06e-6	1/k
Heat capacity at constant pressure	710	J/(Kg*k)
Density	4940	Kg/m^3
Young's modulus	105e9	Pa
Possion's Ratio	0.33	

Table 6 Property of Carbon fiber

Property	Value	Unit
Heat capacity at constant pressure	1000	J/(Kg*k)
Density	1200	Kg/m^3
Thermal Conductivity	0.2	W/(m*k)

3.6 RC circuit model

Figure 21 shows the equivalent RC circuits [37]. The RC circuit of the planar electrodes are derived from literature [37]. The RC equivalent circuit of the VACNF was experimentally measured using a chemical analyzer instrument in electrochemical impedance mode. Circuits (a) show the RC with growth media solution without cell. Cp is the double layer capacitance. Rp represents the resistance combined with Warburg impedance and charge transfer resistance (Rct). Warburg impedance is reported as the impedance related to mass diffusion process occurring in the electrode electrolyte interface [37]. The expression of Warburg impedance is show as:

$$Z_w = \frac{\omega^{-\frac{1}{2}} K_\omega}{A_e(1+j)}$$

A_e is the electrode area and K_ω (Ω sec$^{-1/2}$cm^2) is a constant determined by the electrochemistry and mobility of the ions involved in the charge transfer reaction. Charge transfer resistance (R_{ct}) represent the electron transfer rate at the interface:

$$R_{ct} = \frac{V_t}{J_0 Z}$$

V_t is the thermal voltage (KT/q) where K is Boltzmann's constant, T is the temperature and q is the charge on an electron and is 25mV at room temperature. j_0 is the exchange current density (A/cm^2) and Z is the valence of ion involvedin the charge transfer reaction.

Rs is the spreading resistance, which effects of the spreading of current from localized electrode to a distant counter electrode in the solution. The solution resistance is determine by:

$$Rs = \frac{\rho L}{A}$$

ρ is the resistivity of the electrolyte, L is the length between sensing and counting electrodes, and A is the cross-sectional area of the solution through which the current passes. For the coplanar electrode model, Rp = 50Ω, Cp = 1nF and

Rs = 1kΩ. The value for Cp and Rs are beads on literature [37]. And for Rp, the value was set to 50Ω, which is very low value to represent the resistance of gold layer. For VACNF model, Rp = 446Ω, Cp = 1nF and R_{gap} = 100k. The value of each elements are based on experimental results using a chemical analyzer in electrochemical impedance mode. For the cell model Rc = Rp/A, where A is the ratio between the surface area that cell are covering and the surface area of the electrode and VACNF [37]. In this simulation A is assumed to be 0.5 in both models for a fair comparison. By running AC analysis in SPICE on coplanar electrode model and VANCF model, the impedance could be quantified after comparing the impedance changes between the cell and without cell for both model. The VACNF model shows a larger impedance change than the coplanar electrode model for input frequency is under 10-100 KHz range. Figure 22 shows simulation result for impedance differences between with cell and without cell for both the VACNF model coplanar electrode model. The coplanar electrodes show an impedance change of 200Ω in going form no cell adhered to a cell adhered. The VACNF electrode shows a ~500Ω change in going from no cell to cell adhered. This proves that the VACNF electrodes are more sensitive than coplanar electrodes. However, this is at the expense of the frequency response. The VACNF show an earlier frequency roll off than the coplanar electrodes by an order of magnitude (10kHz vs 300kHz).

(a) RC Model without cell   (b) RC Model with cell
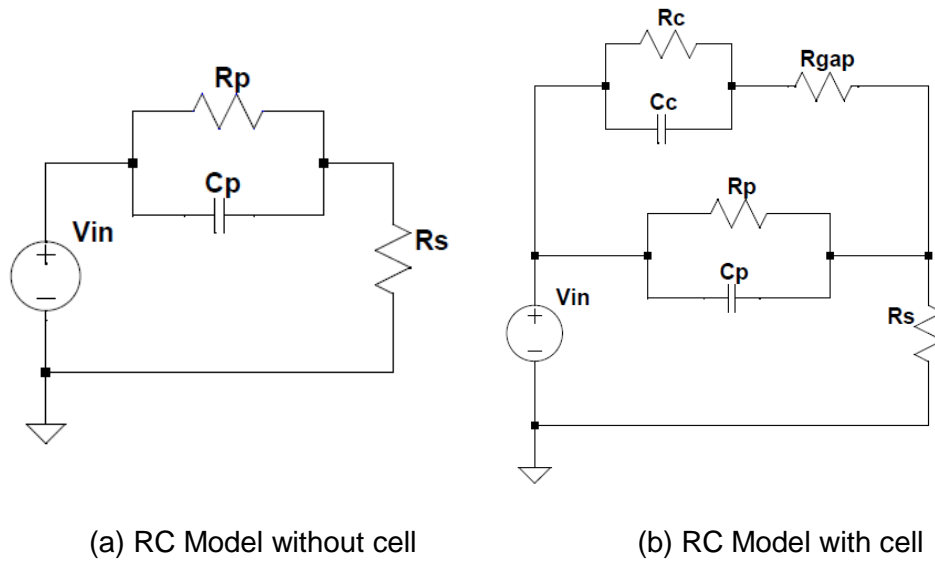
Figure 21. Equivalent RC Circuits Model
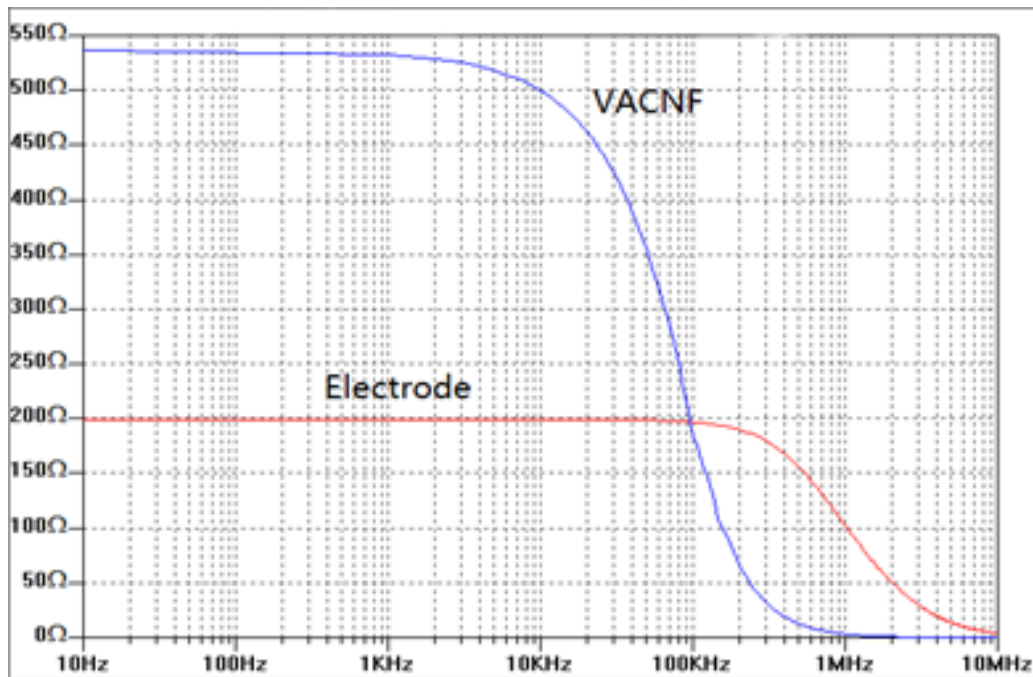
Figure 22. Impedance difference with cell and without cell for VACNF model coplanar electrode model

CHAPTER 4
MEASUREMENT SYSTEM SETUP AND CELL CULTURE

4.1 Measurement System Setup

A custom cell impedance electronic readout measurement system was designed using a lock-in amplifier to create a reference signal and collect the output signal. Figure 23 shows the system setup. The Quartz sample is connected via leads to a resistor in series with a voltage source. The lock in is used to measure the voltage across the electrodes. The VACNF are surrounded by a well to hold the cell culture and its growth medium.
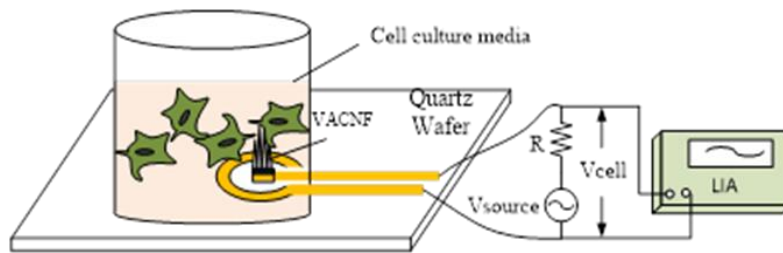
Figure 23. Cell impedance measurement system
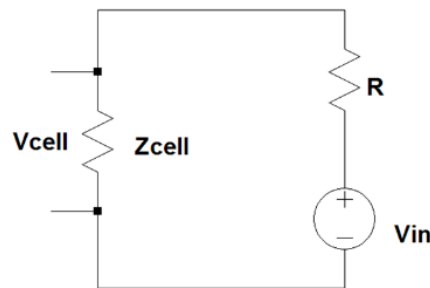
Figure 24. Simplified RC Equivalent Circuits

Instead of measuring the cell impedance directly, the system measures the voltage across the cell. Figure 24 shows the circuit diagram of the equivalent circuit. V_{in} is the same as Vsource from Figure 23. V_{in} and R act as a current source. By apply Ohms low and voltage division theory, the impedance of cell, Zcell is able to be calculated from the measured Vcell. The expression of impedance calculated is shown as:

$$V_{source} = V_{cell} + V_R$$

$$V_{cell} = I * Z_{cell}$$

$$Z_{cell} = \frac{V_{cell}}{I} \qquad I = \frac{V_R}{R}$$

$$Z_{cell} = V_{cell} / (\frac{V_R}{R})$$

$$Z_{cell} = \left(\frac{V_{cell}}{V_{source} - V_{cell}} \right) * R$$

V_{cell} and V_{source} are recorded by a custom Matlab program through a data acquisition card. A reference resistor, R = 8.1k, acts as a source to limit the current (below 1mA) flowing through the cell, which is low enough to not kill the cells. Figure 25 shows a picture of the measurement system, it shows the lock in amplifier, the laptop, an interface board (c) and the connector to the VACNF sample electrodes (d).

For doing measurement, a Matlab program was developed to active the lock-in amplifier and recorded the data. Using Lock-in amplifier as voltage source, which is able to create an input signal with different frequency. And also use lock-in amplifier to measure the voltage accrues cells, which is Vcell that shows on the equation above. A printed circuit board (PCB) board (Figure 24 c) was designed to switch the measurement units on the VACNF platform. A connector (d) allow to attach the VACNF platform to measurement system. This connector can also be used to connect the commercial array systems.
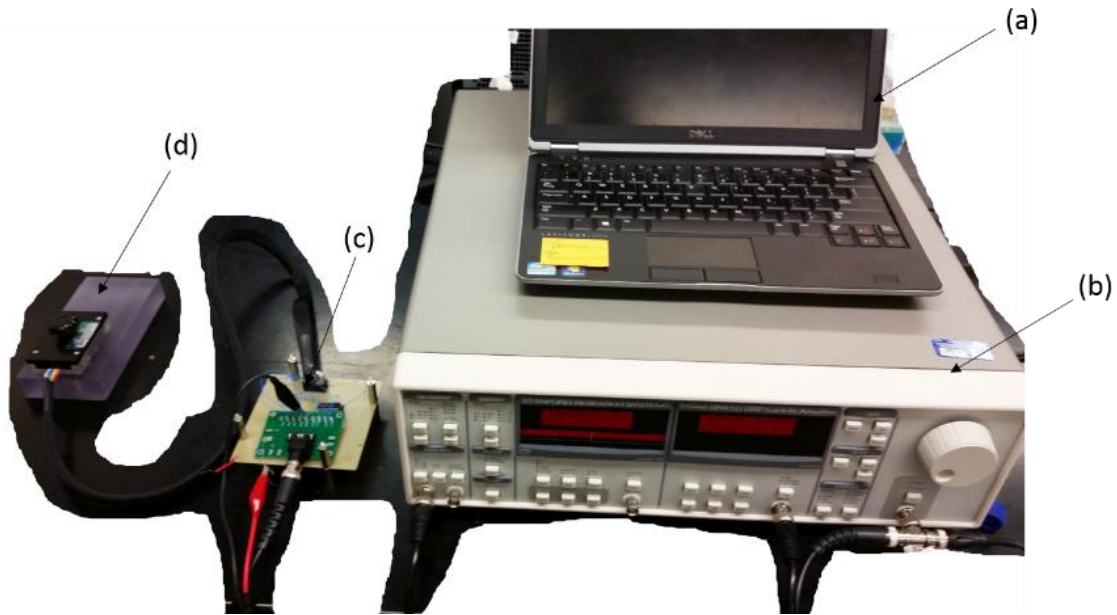
Figure 25. Equipment using in Measurement
(a) Laptop (b) lock-in amplifier (c) PCB connector (d) connector
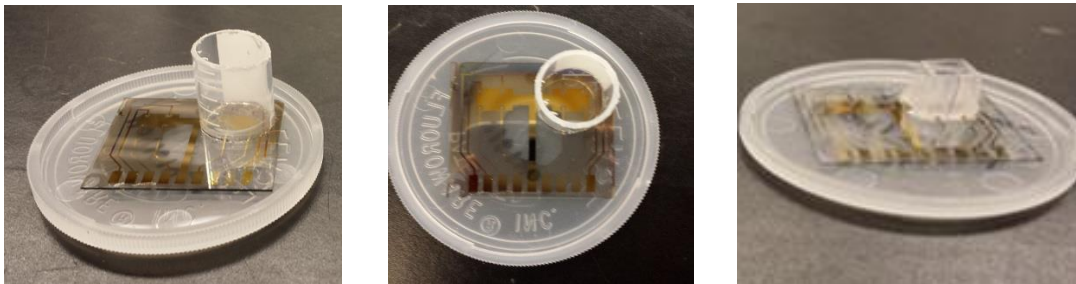
Figure 26. Platforms used in Measurement

During the measurement, cells were placed inside of a plastic well as figure 26 shows. The maxima capacity of well is 1.5 mL. During our measurement, 1 mL of solution was placed in the well. The well is made of culture grade centrifuge tubes, and are thus biocompatible. The epoxy used to "glue" the well to the sample is also biocompatible.

4.2 Cell Culture Equipment and Process

Cell culture plays an important role in this project. In order to measure cell impedance, healthy live cells are a necessary factor. Bovine Aortic Smooth Muscle cells were used in our preliminary experiments. These cells were purchased from Cell Applications Inc. in T25 proliferating flasks. Figure 27 shows the tools and equipment that are used in cell culture. The figure 27 shows the T25 cell culture flasks, cell scrapers, pipettes, aspirators and growth media used in culturing the cells.
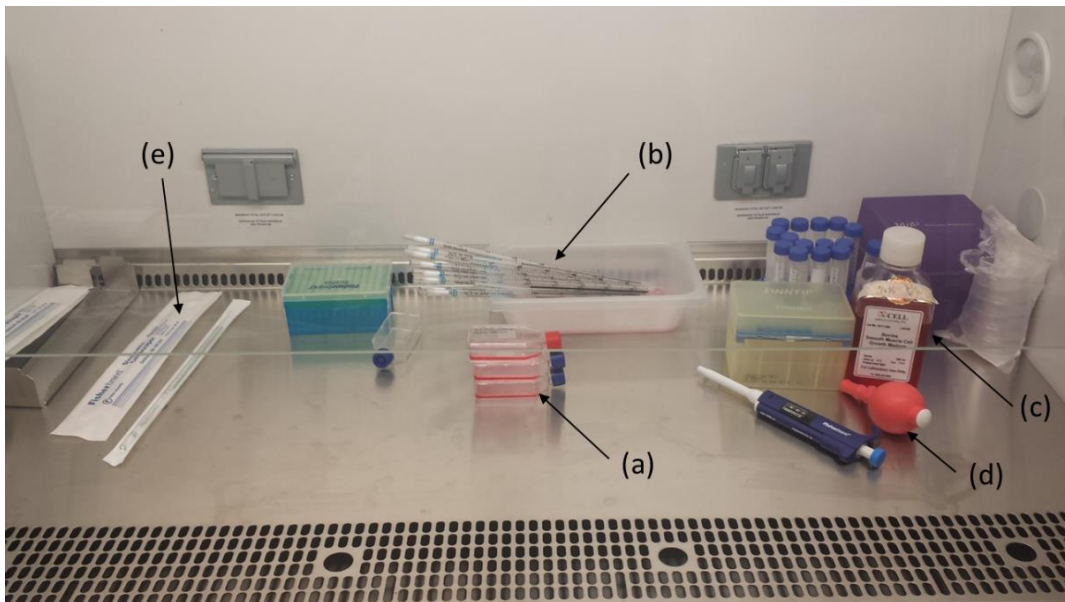
Figure 27. Tools and Equipment used in Cell Culture
(a) Cell culture flasks, (b) pipettes, (c) cell growth media, (d) rubber ball aspirator, (e) cell scraper

In order to keep the cells alive and healthy, cells were kept in an incubator. The condition of incubator was set to 37°C and 5% CO_2, which is the ideal condition for cells' growth [38]. The growth media is changed every 2-3 days once the cells have reached approximately 80% confluence. 5mL of media was added

to each T25 flask to give enough nutrient for cells. Subculture flask every week. All the processes have been done in a disinfected biosafety operation hood under strict aspectic conditions.

The cell culture steps for culturing a population of cells in a T25 flask are outlined below:

- Disinfect equipment and working area using 70% alcohol solution
- Move cell flasks from incubator to biosafety hood
- Remove growth media using pipettes from flask and place to waste liquid container
- The used pipettes should be placed in waste container
- Add 5 ml fresh growth media to flask
- Disinfect the outside of flask and place it to incubator

4.3 Cell Subculture and Plating to VACNF

In order to measure the cell impedance, cells have to be moved from flasks and placed in to the testing platform. Cell sub-culturing technique was applied in this process. As a first attempt, cell scrapers were used. The specific steps are described below:

- Remove growth media
- Add 5ml HBSS to flask
- Remove HBSS
- Add 2ml growth media
- Using cell scraper to scratch bottom of flask gently
- Remove cell suspension onto VACNF sample

However, after this process, all the cells were squeezed together and become a big "cell ball". Usually cells need at least 1 week to separate evenly. Also the space on the measurement is very limited, only able to contain 1 ml growth media

in the well (image shows on figure 26). Therefore the cells find it difficult to survive in such a limited space.

Instead of using cell scraper, trypsin was used subculture the cells instead. The procedure is outlined below:

- Remove growth media
- Add 5ml HBSS to flask
- Remove HBSS
- Add 2ml trypsin
- Place flask in incubator (5 min)
- Tap gently at underside of flasks. Cell will flowing in the media
- Add 2ml of growth media
- Move the cell suspension to a centrifuge tube
- Spin down using centrifuge
- Remove supernatant
- Add 2ml of media
- Put 1ml onto sample

This process significantly increased viability, and results in a not "too large" and not "too small" population of cells on the VACNF samples. The purpose of trypsin is to force cells to isolate from flask bottom. Trypsin is an enzyme which has a function of dissolving protein. The reason of cell could stick on the flask is there is a thin protein layer between the cells and the flask surface. This thin layer of protein works as a layer of "glue" and keeps the cells adhered on the bottom of the flask. Trypsin will dissolve this protein layer and force the cells to float within the growth media. Similarly, trypsin also could dissolve protein in the cells and kill the cells if left for too long. However, trypsin will be inhibited when mixed with the growth media. The growth media contains plasma, amino acids and nutrients for the cells. By using this process, we were able to isolate individual cells from growth flasks and place cells onto the testing platform. This technique increased the success rate of measurement. Figure 28 shows the cells that cultured directly on VACNF platform. The Black circle in the middle is the VACNF array. As the image shows

41

cells are evenly distributed on the VACNF array. When healthy these cells are elongated in shape. Unviable or dead cells show a rounded morphology. We were able to culture cells for up to 1 week on these VACNF samples as confirmed by visual microscope observation.
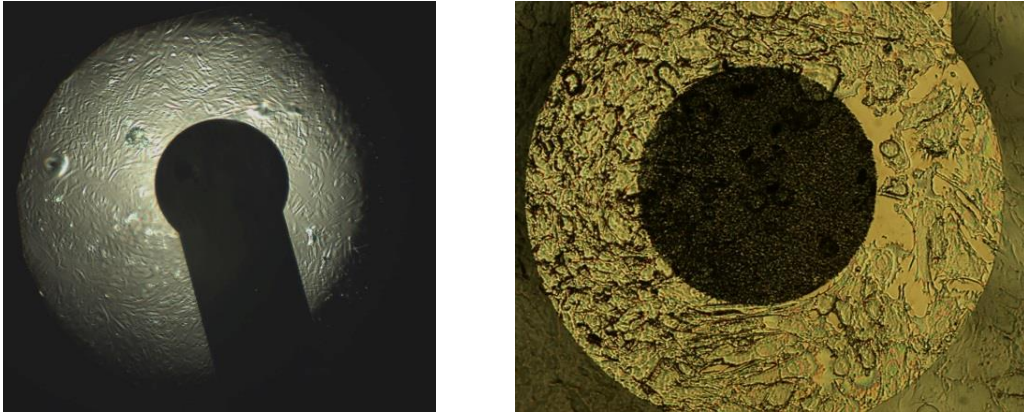
Figure 28. Image of Confluent Layer of Cells Cultured Directly on VACNF Array

CHAPTER 5
MEASUREMENT RESULTS USING VACNF PLATFORM

5.1 System testing using RC circuits

For calibrating the system, we utilized an RC circuit array with our system. A RC circuit test array was used as a measuring object, instead of electrode platform shows on figure 29. There are 8 different sets of RC circuits. The Value for each resistances are show on table 7. For each well, there is a resistor series with a capacitor and anther resister is paralleled with resistor and capacitor.
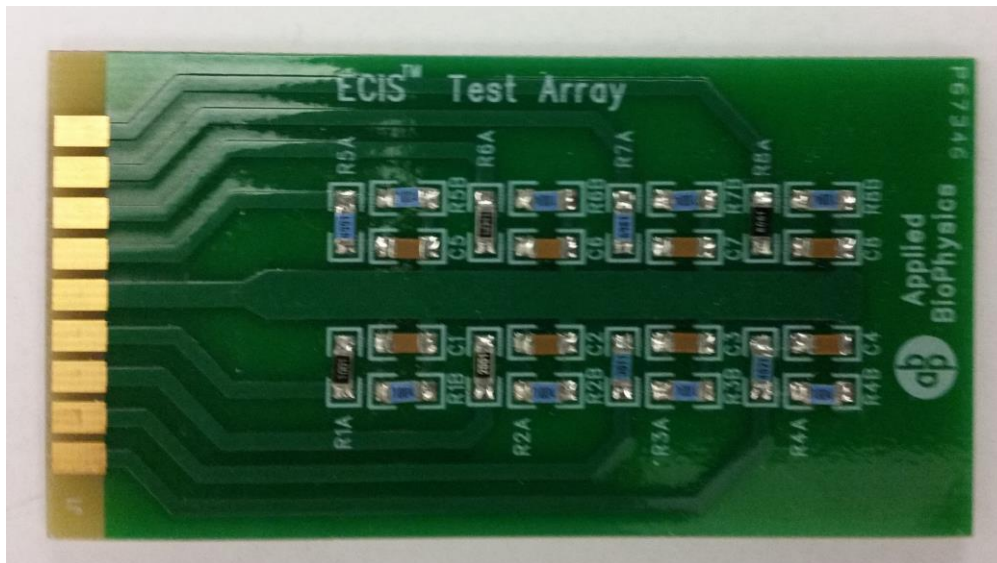
Figure 29. Applied Biophysics Test Array

Table 7 Resistance and Capacitance Value on Test Array

Well Number	Resistance (Ω)	Capacitance (μf)
1	1000	10
2	2000	10
3	3000	10
4	4000	10
5	5000	10
6	6000	10
7	7000	10
8	8000	10
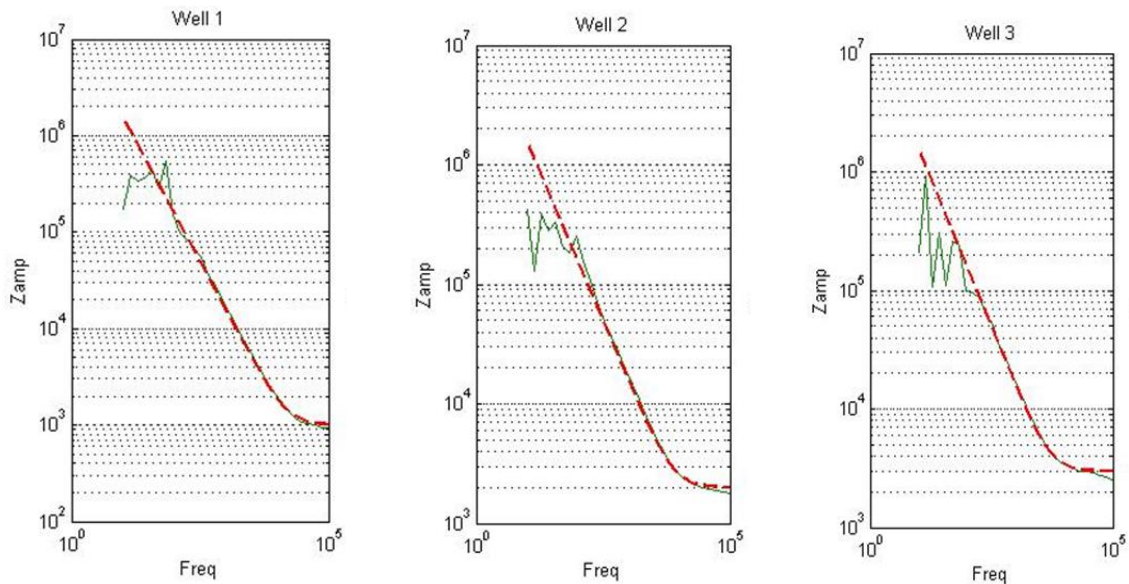
Figure 30. Measurement Results for RC Board

The measurement results for first three wells are shown in Figure 30. The dashed line shows the theoretical result by using Matlab to simulate. The back lines show the measurement results. From the figures it is obvious that on the high frequency range, our system shows very accuracy matchup between measurement results and theoretical simulation results. However, for the low

44

frequency range measurement show huge differences. The mismatch at low frequency range is due to the limitation of lock-in amplifier. In the lower frequency range, as one of the characteristic of RC circuits, is it shows larger impedance. The impedance value is calculated by

$$Z_{RC} = \left(\frac{V_{Rc}}{V_{source} - V_{RC}} \right) * R$$

R and V_{source} are constant numbers. So, in the lower frequency V_{RC} shows as a very large voltage and for higher frequency it shows as a smaller voltage value. However, as a one limitation of this lock-in amplifier, we have to set the sensitivity of lock in amplifier manually before the measurement.

5.2 Measurement for Different Objects with Multiple Frequencies

Figure 31 shows measurement result for different objects with different frequency.

Figure 31. Impedance for Different Objects with Multiple Frequency

45

In this measurement, we measured the impedance for air, which is an open circuit, cell growth media and growth media with cell solution. The impedance of growth media with cell was measured right after the cell suspension was placed on the VACNF platform. Thus, there will be very little differe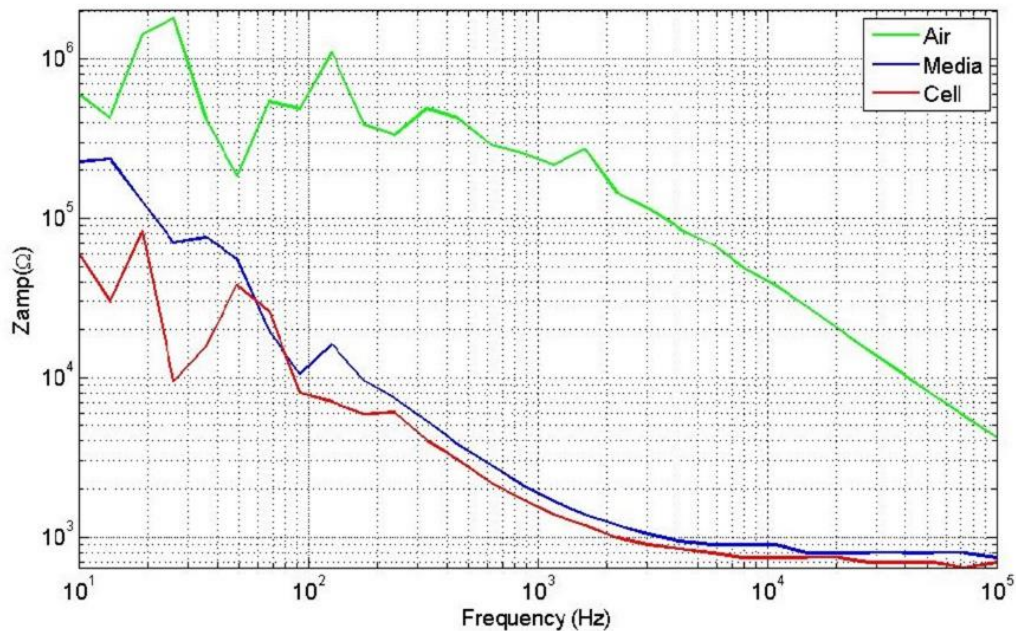nce between measuring the growth media and the growth media with suspended cells. During all measurements, the VACNF platform was placed in the incubator, with set conditions as 37°C and 5% CO_2 level. All three objects were measured by same measurement units. As the result, open circuit shows the largest impedance in all frequency ranges. Cell and growth media solution shows a small amount of decrease in impedance value compared with growth media only. This measurements result shows that whole measurement system was functional, and the system is able to measure the impedance of different objects. Also this result shows that our system has good stability with input frequency over 500Hz.

5.3 A long term impedance measurement

In this measurement, the impedance change in the bovine cells were observed for a longer time period. The test was continuously running for 500 min for monitoring and recording the impedance change of cell media solution. Two tests results are shown in Figure 32. Two different VACNF platform sample were used in the two experiments. During the whole measurement period, the VACNF sample was placed in the incubator to keep the cells alive. The input frequency was set to 2 kHz. From the measurement result shows above. Our system has good stability for input frequency over 500 Hz. And also as the results shows, in 2 kHz, the impedance for different object shows largest difference with 2-5k Hz input frequency.

The measurements results show that before 150 min, impedance increases in both tests. This is because, during this time period, cells are starting to precipitate in growth media, and are starting to settle, first via gravity and then via

biophysical chemical processes, onto the VACNF. After 200 min, most of the cells floating in the growth media are adhered to the VACNF and the impedance stays at a constant level. This measurement results proves that our measurement system is able to measure the impedance change in real time. It also shows that it has stable performance in long term measurement.
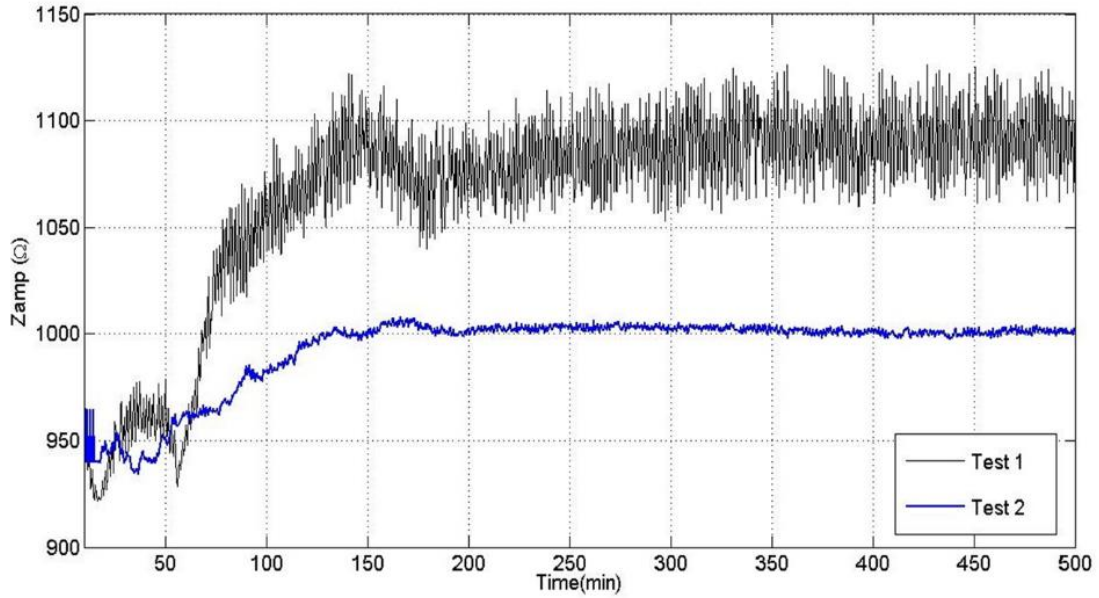

Figure 32. Long Period Measurement for Impedance Changing

CHAPTER 6
CONCLUSION AND FUTURE WORK

In conclusion, we have demonstrated the first electrical cell impedance measurement system using vertically aligned carbon nanofibers. Because of the unique structure of VACNFs, using VACNFs improved the sensitivity of the measurement system compared to the traditional coplanar electrodes. The nanofibers were deterministically grown and the system has been verified in real time impedance measurements of biological cells adhering to the electrodes. Physical device simulation using COMSOL and equivalent RC circuits modeling have shown that the nanofibers have significant contribution for electrical field distribution. As a result, nanofibers increase the electrical potential compared with traditional planar electrodes. This will increase the sensitivity of the measurement. Thus, this work has expanded the possibilities of VACNF applications in biosensing.

Future work includes improving the process of adding the passivation layer. As shows previously, after place a passivation layer, a significant arcing damage shows on platform and damage the interconnection. This process will help to analysis and understanding the effects and principle of VACNF in bio-sensing. Furthermore, as a lab-on chip or portable application, the system need to be integrated on a smaller scale. The current implementation uses a large lock in amplifier. This amplifier can only measure on well at a given time, and can only measure one frequency at a time. Thus, even though the resolution of the system can be significantly increased using the nanofibers, the measurement speed will be extremely slow. One possible solution is to replace the lock-in amplifier with a custom integrated circuit chip where the system would be able to measure different measurement units and multiple frequencies at same time for high speed high throughput measurements.

LIST OF REFERENCES

[1] J.Wegener, "Electric Cell-substrate Impedance Sensing as a Nonivasive Means to Montior the Kinetices of cell Spreading to Artifical Sureface," *Expeermental Cell Re,* vol. 259, no. 1, pp. 159-166, 2000.

[2] "Applied biophysics," Applied biophysics,Inc, 2015. [Online]. Available: http://www.biophysics.com/cultureware.php.

[3] S. E. McNeil, "Nanotechnology for the biologist," *Journal of Leukocyte Biology,* vol. 78, no. 3, pp. 585-594, 2005.

[4] F. I. J.M.Corres, "High Senstivity Optical Fiber pH Snsor using poly (acrylic acid) nanofibers," *IEEE,* vol. 978, no. 1, pp. 4673-4642, 2013.

[5] X. G. H.Liu, "Electrospun Nickel Oxide Nanofiber for Gas Sensor Application," *IEEE,* vol. 978, no. 1, 2013.

[6] K. S.U.Kim, "Carbon Nanofiber Compoistes for the Electrodes of Electrochemical Capacitor," *Chem.Phys.Lett,* vol. 400, no. 1-3, pp. 253-253, 2004.

[7] Jyongsik Jang, onwon Baea, Moonjung Choia, Seong-Ho Yoonb, "Fabrication and characterization of polyaniline coated carbon nanofiber for supercapacito," *Carbon,* vol. 43, no. 12, pp. 2730-2736, 2005.

[8] Ole Waldmanna, Arun Persauda, Rehan Kapadiab, Kuniharu Takeib, Frances I. Allena, c, Ali Javeyb, Thomas Schenkela, "Effects of palladium coating on field-emission properties of carbon nanofibers in a hydrogen plasma," *Thin Solid Films,* vol. 534, pp. 466-491, 2013.

[9] Ivar Giaever, Charles R. Keese, "Electric Cell-Substrate Impedance Sensing Concept to Commercialization," in *Electric Cell-Substrate Impedance Sensing and Cancer Metastasis*, Springer, 2012, pp. 1-19.

[10] Reddy L, Wang H, Keese CR, Giaever I, Smith T, "Assessment of rapid morphological changes associated with elevated cAMP levels in human orbital fi broblasts," *Exp Cell Res ,* vol. 245, pp. 360-367, 1998.

[11] Lavanya Reddy, Hwai-Shi Wang,harles R. Keesea, Ivar Giaevera, Terry J. Smithb,, "Assessment of Rapid Morphological Changes Associated with Elevated cAMP Levels in Human Orbital Fibroblasts," *Experimental Cell Research,* vol. 245, no. 2, pp. 360-367, 1998.

[12] Kamon Kawkitinarong, Laura Linz-McGillem, Konstantin G. Birukov, and Joe G. N. Garcia, "Differential Regulation of Human Lung Epithelial and Endothelial Barrier Function by Thrombin," *Cell Mol.Biol.,* vol. 32, pp. 517-527, 2004.

[13] A.M. Malek and S. Izumo, "Mechanism of endothelial cell shape change and cytoskeletal remodeling in response to fluid shear stress," *Journal of Cell Scince,* vol. 109, pp. 713-726, 1996.

[14] Jurgen F. Vanhauwe,Tarita O. Thomas, Richard D. Minshall, Chinnaswamy Tiruppathi, Anli Li, Annette Gilchrist, Eun-ja Yoon, Asrar B. Malik and Heidi E. Hamm, "Thrombin Receptors Activate Go Proteins in Endothelial Cells to Regulate Intracellular Calcium and Cell Shape Changes," *The Journal of Biological Cheistry,* vol. 277, pp. 34143-24149, 2002.

[15] Jamie H. Rosenblum Lichtenstein, Ramon M. Molina, Thomas C. Donaghey, Chidozie J. Amuzie, James J. Pestka, Brent A. Coull and Joseph D. Brain, "Pulmonary Responses to Stachybotrys chartarum and Its Toxins: Mouse Strain Affects Clearance and Macrophage Cytotoxicity," *Tocicological and Its Sciences,* vol. 116, pp. 113-121, 2010.

[16] Sungbo Cho and H Thielecks, "Electrical characterization of human mesenchymal stem cell growth on microelectrode," *Microlctronic Engineering,* vol. 85, pp. 1272-1274.

[17] John H. T. Luong, Mehran Habibi-Rezaei, Jamal Meghrous, Caide Xiao, Keith B Male, and A. Kamen, " Monitoring Motility, Spreading, and Mortality of Adherent Insect Cells Using an Impedance Sensor," *Analytical chemistry,* vol. 73, pp. 1844-1848, 2001.

[18] Cornelia Hildebrandt, Heiko Büth, Sungbo Cho, Impidjati, and H. Thielecke, "Detection of the osteogenic differentiation of mesenchymal stem cells in 2D and 3D cultures by electrochemical impedance spectroscopy," *Journal of Biotenchnology,* vol. 148, pp. 83-90, 2010.

[19] Sungbo Cho, Erwin Gorjup, and H. Thielecke, "Chip-based time-continuous monitoring of toxic effects on stem cell differentiation," *Annals of Anatomy - Anatomischer Anzeiger,* vol. 191, pp. 145-152, 2009.

[20] S. N. Bhatia, U. J. Balis, M. L. Yarmush, and M. Toner, "Effect of cell-cell interactions in preservation of cellular phenotype: cocultivation of hepatocytes and nonparenchymal cells," *The FASEB Journal,* vol. 13, pp. 183-1990, 1999.

[21] Celeste M. Nelson and Christopher S. Chen, "Cell-cell signaling by direct contact increases cell proliferation via a PI3K-dependent signal," *FEBS Letters,* vol. 514, pp. 238-242, 2002.

[22] Ivar Giaever and C. R. Keese, "Use of Electric Fields to Monitor the Dynamical Aspect of Cell Behavior in Tissue Culture," *IEEE Transactions on Biomedical Engineering,* vol. 33, pp. 242-247, 1986.

[23] Nicholas N. Watkins, Supriya Sridhar, Xuanhong Cheng, Grace D. Chen, Mehmet Toner, William Rodriguez, et al., "A microfabricated electrical differential counter for the selective enumeration of CD4+ T lymphocytes," *Lab on a Chip,* vol. 11, pp. 1437-1446, 2011.

[24] S. K. Mohanty, S. K. Ravula, K. L. Engisch, and A. B. Frazier, "A micro system using dielectrophoresis and electrical impedance spectroscopy for cell manipulation and analysis," in *international Confrenece on Tansducers,Solid-state sensors, Actucators and Microsystem*, 2003.

51

[25] C. Charmnber and T. Hugehes, "Manufacture of Carbon Filmaments". US Patent 405,480, 1889.

[26] L.V.Radushkevich, V.M.Lukyanovich and F. Zh.Patent 26, 1952.

[27] L.C. Chena, C.Y. Yangb, D.M. Bhusarib, K.H. Chena, b, M.C. Linc, J.C. Linb, T.J. Chuangb, "Formation of crystalline silicon carbon nitride films by microwave plasma-enhanced chemical vapor deposition," *Diamond and Related Materials,* vol. 5, no. 3-5, pp. 514-518, 1996.

[28] A. V. Melechko, V. I. Merkulov, T. E. McKnight, M. A. Guillorn, K. L. Klein, D. H. Lowndes and M. L. Simpson, "Vertically aligned carbon nanofibers and related structures: Controlled synthesis and directed assembly," *Journal of Applied Physics,* vol. 97, 2005.

[29] M. A. Guillorn, A. V. Melechko, V. I. Merkulov, E. D. Ellis, C. L. Britton, M. L. Simpson, D. H. Lowndes and L.R.Baylor, "Operation of a gated field emitter using an individual carbon nanofiber cathode," *Applied Physics Letter,* vol. 79, no. 21, p. 3506, 2001.

[30] Martha L. Weeksa, Touhidur Rahmanb , Paul D. Frymiera, Syed K. Islamb, Timothy E. McKnight, "A reagentless enzymatic amperometric biosensor using vertically aligned carbon nanofibers (VACNF)," *Sensors and Actuators B: Chemical,* vol. 133, no. 1, pp. 53-59, 2008.

[31] Ashraf B. Islam, Fahmida S. Tulip, Syed K. Islam, Touhidur Rahman, Associate, and Kimberly C. MacArthur, "A Mediator Free Amperometric Bienzymatic Glucose Biosensor Using Vertically Aligned Carbon Nanofibers (VACNFs)," *IEEE, Snsors Journal,* vol. 11, no. 1, pp. 2798-2804, 2011.

[32] Zhe Yu , Timothy E. McKnight , M. Nance Ericson , Anatoli V. Melechko ,Michael L. Simpson, and Barclay Morrison , "Vertically Aligned Carbon Nanofiber Arrays Record Electrophysiological Signals from Hippocampal Slices," *Nano Letters,* pp. 2188-2195, 2007.

[33] Emily Rand, A.Periyakaruppan, Z,Tanake.etc, "A caron nanofiber based biosensor for simultaneous detection of dopamine and serotonin in the presence of asorbiced," *Biosensors and Bioelectronics,* vol. 42, pp. 434-438, 2913.

[34] A. Kual, "Carbon nanofiber switches and sensors," in *Frequency Control Symposium (FCS), 2012 IEEE International*, Baltimore, MD, 2012.

[35] H. Cui, X. Yang, L. R. Baylor and D. H. Lowndes, "Growth of multiwalled-carbon nanotubes using vertically aligned carbon nanofibers as templates/scaffolds and improved field-emission properties," *Applied Physics Letter,* vol. 86, 2005.

[36] B. Hafner, "Energy Dispersive Spectroscopy on the SEM:Aprimer," [Online]. Available:
http://www.charfac.umn.edu/instruments/eds_on_sem_primer.pdf.

[37] Alberto Yufera, Ablerto Olmo, Paula Daza and Daniel Cente, "Cell Biometerics Based on Bio-Impedance Measurements," in *Advanced Biometric Techologies*, pp. 343-363.

[38] R. I. Freshney, Culrure of Animal Cells, New Jersy: John and Sons, Inc, 2010.

[39] M. J. N. Riguad B, "Bioelectrical impedance techniques in medicine. Part I: Bioimpedance measurement. Second section: impedance spectrometry," *Critical Reviews in Biomedical Engineering [,* pp. 257-351, 1996.

VITA

Yongchao Yu was born in Shenyang, China. When he was 4 years old, he moved to Japan with his family. In 1999, he and his family back to Beijing, China. In 2008, after he graduated from high school in Beijing, he came to the US and started his undergraduate study in Electrical Engineering at the University of Tenseness, Knoxville. After he graduated from UTK, he continued his masters study at UTK in August 2013. In 2015, he finished his thesis research under the advice of Dr. Nicole McFarlane.